IMPURITY EFFECTS AND SYMMETRY OF THE ORDER PARAMETER IN HIGH-TEMPERATURE OXIDE SUPERCONDUCTORS

A THESIS
SUBMITTED TO THE DEPARTMENT OF PHYSICS
AND THE INSTITUTE OF ENGINEERING AND SCIENCE
OF BILKENT UNIVERSITY
IN PARTIAL FULFILLMENT OF THE REQUIREMENTS
FOR THE DEGREE OF
MASTER OF SCIENCE

By
Mehmet Bayındır

September 1997

QC
612
.S8
B39
1997

IMPURITY EFFECTS AND SYMMETRY OF THE ORDER PARAMETER IN HIGH-TEMPERATURE OXIDE SUPERCONDUCTORS

A THESIS

SUBMITTED TO THE DEPARTMENT OF PHYSICS

AND THE INSTITUTE OF ENGINEERING AND SCIENCE

OF BILKENT UNIVERSITY

IN PARTIAL FULFILLMENT OF THE REQUIREMENTS

FOR THE DEGREE OF

MASTER OF SCIENCE

Mehmet Bayındır

tarafından bağışlanmıştır

By

Mehmet Bayındır

September 1997

QC
612
.S8
B39
1997
BC38365

I certify that I have read this thesis and that in my opinion it is fully adequate, in scope and in quality, as a dissertation for the degree of Master of Science.

Assist. Prof. Zafer Gedik (Supervisor)

I certify that I have read this thesis and that in my opinion it is fully adequate, in scope and in quality, as a dissertation for the degree of Master of Science.

Prof. Igor O. Kulik

I certify that I have read this thesis and that in my opinion it is fully adequate, in scope and in quality, as a dissertation for the degree of Master of Science.

Assoc. Prof. Recai Ellialtıoğlu

Approved for the Institute of Engineering and Science:

Prof. Mehmet Baray,
Director of Institute of Engineering and Science

Abstract

IMPURITY EFFECTS AND SYMMETRY OF THE ORDER PARAMETER IN HIGH-TEMPERATURE OXIDE SUPERCONDUCTORS

Mehmet Bayındır
M. S. in Physics
Supervisor: Assist. Prof. Zafer Gedik
September 1997

Identification of the symmetry of the order parameter (OP) of high-T_c cuprates is important because it helps to understand possible mechanism that govern the physics of these materials. However, up to now, there is no consensus on the symmetry of the OP. On the other hand, nonmagnetic impurity substitutions would test the symmetry of OP. Present theoretical calculations overestimate suppression of the critical temperature (by a factor of 2 or more) in comparison to the experimental data. So far, differences between zinc (Zn) and nickel (Ni) substitutions have not been well understood. Considering the above arguments, effects of nonmagnetic impurities on the high-temperature cuprates are investigated by solving the Bogoliubov-de Gennes (BdG) equations on two-dimensional square lattice. The critical impurity concentration is found to be very close to the experimental values. Possibility of extracting the symmetry of OP from the obtained results is discussed. Finite-ranged impurity potentials and different potential strengths for different impurities are proposed to explain differences between Zn and Ni substitutions. Finally, it is concluded that our results are in favor of d-wave symmetry for tetragonal and

s+d-wave symmetry for orthorhombic phase, and explain quite well the effects of nonmagnetic impurity substitutions in the high-T_c oxide superconductors. Beside these, the physical properties of the high-temperature oxide superconductors, the BdG equations and effects of nonmagnetic impurities on isotropic and anisotropic superconductors are reviewed.

Keywords: Superconductivity, order parameter, impurity substitution, high-temperature superconductivity, critical temperature suppression, s-wave, d-wave, d+s-wave, Zn or Ni-Cu substitution

Özet

YÜKSEK-SICAKLIK OKSİT ÜSTÜNİLETKENLERİNDE SAFSIZLIK ETKİLERİ VE DÜZEN PARAMETRESİNİN SİMETRİSİ

Mehmet Bayındır
Fizik Yüksek Lisans
Tez Yöneticisi: Yrd. Doç. Dr. Zafer Gedik
Eylül 1997

Yüksek-sıcaklık üstüniletkenlerde düzen parametresinin simetrisinin kesin olarak tespit edilmesi, bu malzemelerin fiziği hakkında bilgi verecek olması açısından önemlidir. Fakat günümüze kadar yapılan çalışmalarda, düzen parametresinin simetrisi hakkında kesin bir sonuca varılamamıştır. Öte yandan, safsızlık etkileri, düzen parametresinin simetrisinin tespitinde yardımcı olabilir. Şimdiye kadarki teorik hesaplamalar, safsızlıklardan dolayı, kritik sıcaklıktaki azalmayı deney verilerine göre en az iki kat daha yüksek bulmaktadır. Ayrıca, çinko ve nikel safsızlıkları arasındaki fark henüz tam olarak anlaşılamamıştır. Bu çalışmada, Bogoliubov-de Gennes (BdG) denklemleri iki-boyutlu kare örgü üzerinde çözülerek manyetik olmayan safsızlıkların yüksek-sıcaklık oksit üstüniletkenleri üzerindeki etkileri incelendi. Sonuçlardan sistemin düzen parametresinin çıkarılıp çıkarılamayacağı tartışıldı. Kritik safsızlık konsantrasyonu deney verilerine çok yakın bulundu. Sonuçlar, tetragonal faz için d-dalgasını ve ortorombik faz için d+s-dalgasını desteklemekte ve manyetik olmayan safsızlıkların yüksek-sıcaklık oksit üstüniletkenleri üzerindeki etkilerini tutarlı şekilde açıklamaktadır. Ayrıca; yüksek-sıcaklık oksit üstüniletkenlerinin, BdG denklemlerinin, manyetik

ve manyetik olmayan safsızlıkların isotropik ve isotropik olmayan üstüniletkenler üzerindeki etkilerinin kısa bir özeti yapıldı.

Anahtar
sözcükler: üstüniletkenlik, düzen parametresi, safsızlık katma, yüksek-sıcaklık üstüniletkenliği, kritik sıcaklık azalması, s-dalgası, d-dalgası, d+s-dalgası, Cu yerine Zn veya Ni katma

Acknowledgement

It is my pleasure to express my deepest gratitude to my supervisor Assist. Prof. Zafer Gedik for his guidance, helpful suggestions and fruitful discussions throughout my thesis works. I have not only benefited from his wide spectrum of interest in physics but also learned a lot from his superior academic personality.

I would like to thank to all members of physics department especially my friend Çetin Kılıç for his valuable comments, and making my life joyful and easier.

I wish to express my great thanks to my residence-mates Nasuhi Yurt and Ertuğrul Uysal and my friends Mehmet Orhan, İsmail Ağırman and Ersin Keçecioğlu for their continuous help and moral support.

It is also my pleasure to acknowledge Prof. I. O. Kulik and Assist. Prof. T. Hakioğlu for their valuable discussions.

Finally I would express my endless thank to my family for their understanding and moral support.

Contents

Abstract i

Özet i

Acknowledgement i

Contents i

List of Figures iii

List of Tables vi

1 INTRODUCTION 1

1.1 Low-Temperature Superconductors 1

1.2 High-Temperature Superconductors 2

1.3 Motivations and Outline 4

2 PROPERTIES OF HIGH-TEMPERATURE OXIDE SUPERCONDUCTORS 6

2.1 Normal State Properties 7

2.2 General Properties of Superconducting Phase 9

2.3 Structure of the Cuprates 12

2.3.1 Structure of $YBa_2Cu_3O_{6+x}$ 16

2.4 Pairing Mechanism 17

2.5 Symmetry of the Order Parameter 19

2.6 The Effect of Impurity Substitution in the Basal Plane 22
2.7 Review of Experiments 28

3 ISOTROPIC AND ANISOTROPIC IMPURE SUPERCONDUCTORS 31
3.1 The Self-consistent Field Method: Bogoliubov-de Gennes Equations 31
3.2 Effects of Nonmagnetic Impurities on Isotropic Superconductors 37
3.3 Effects of Nonmagnetic Impurities on Anisotropic Superconductors 40

4 INFLUENCE OF IMPURITY SUBSTITUTIONS ON THE HIGH-TEMPERATURE OXIDE SUPERCONDUCTORS 49
4.1 The Bogoliubov-de Gennes Equations for Two-dimensional Lattice 49
4.2 On the Numerical Solution of BdG Equations 56
4.3 Variation of Order Parameter in the Vicinity of a Single Impurity 60
4.4 Determination of Coherence Length ξ and Critical Temperature T_c 62
4.5 Nonmagnetic Impurity Substitution in High-T_c Cuprates: Experimental Results 67
4.6 Nonmagnetic Impurity Substitution in High-T_c Cuprates: Theoretical Calculations 67
4.7 Nonmagnetic Impurity Substitutions in the High-T_c Cuprates for Various Pairing Symmetry 71
4.7.1 Isotropic s-wave Superconductors 71
4.7.2 d-wave Superconductors 72
4.7.3 s+d-wave Superconductors 74

5 RESULTS AND CONCLUSIONS 76

List of Figures

2.1 Temperature dependence of the resistivity ρ along the three axes of orthorhombic crystals of YBCO. 8

2.2 Temperature dependence of the inverse Hall coefficient $1/R_H$ for $YBa_2Cu_{3-x}Zn_xO_{7-\delta}$ crystal doped with Zn. 9

2.3 The fundamental perovskite unit in the oxide superconductors. 13

2.4 Sketch of the superconducting orthorhombic YBaCuO unit cell. 14

2.5 Schematic lattice structure of the YBCO compounds. 14

2.6 Phase diagram of a cuprate compound ($La_{2-x}Sr_xCuO_4$) as a function of temperature. 15

2.7 Phase diagram of a cuprate compound ($YBa_2Cu_3O_{6+x}$) as a function of temperature. 17

2.8 Dependence of lattice constants, critical temperature and effective valence of $YBa_2Cu_3O_x$ on the oxygen content. 18

2.9 Order parameter symmetries and density of states for different pairing symmetries. 20

2.10 The order parameter $\Delta(0)$, critical temperature T_c and energy gap $\Omega(0)$ are plotted as a function of pair breaking parameter α. 22

2.11 The order parameter $\Delta(T)$ versus temperature for several values of pair breaking parameter α. 24

2.12 Dependence of the T_c on the Zn concentration in $La_{1.8}Sr_{0.2}Cu_{1-x}Zn_xO_4$ and $YBa_2(Cu_{1-x}Zn_x)_3O_{7-y}$. 25

2.13 Lattice parameters and T_c of $YBa_2(Cu_{1-x}\mathcal{M}_x)_3O_{7-y}$ as a function of Zn content and Ga content. 26

2.14 The variation of the lattice parameters a and b and the oxygen content of $YBa_2Cu_{3-x}\mathcal{M}_xO_{7-y}$ as a function of x. 27
2.15 The critical temperature T_c versus dopant concentration x for $YBa_2Cu_{3-x}\mathcal{M}_xO_{7-\delta}$. 28
2.16 Temperature dependence of the depolarization rate σ for $YBa_2Cu_3O_x$ and $Y(Ba_{1-x}La_x)_2Cu_3O_7$. 29
3.1 Dependence of the transition temperature on the pair breaking parameter for different values of the anisotropy χ. 45
3.2 Normalized critical temperature T_c/T_{c0} versus the pair breaking parameter α for d-wave superconductors. 46
3.3 Normalized critical temperature T_c/T_{c0} as a function of the pair breaking parameter α for s+d-wave superconductor for the different values of r. 48
4.1 CuO_2 plane in the high-T_c oxide superconductors. 50
4.2 Plots of order parameters for extended s- and d-wave. 57
4.3 The flow chart describing the computational procedure. 58
4.4 Dependence of the order parameter on number of electrons per lattice site. 59
4.5 Dependence of the order parameter on the strength of the impurity potentials. 60
4.6 Variation of s-wave order parameter in the vicinity of an impurity located at the center of the lattice. 61
4.7 Variation of s+d-wave order parameter in the vicinity of an impurity located at the center of the lattice. 61
4.8 Variation of d-wave order parameter in the vicinity of an impurity located at the center of the lattice. 62
4.9 Variation of d-wave order parameter in the vicinity of an impurity located at the center of the lattice. 63
4.10 Amplitude of $g(0,i)$ for d-wave. 63
4.11 Amplitude of $g(0,i)$ for s+d wave. 64

4.12 Order parameter vanish at the impurity site and recover its bulk values at a distance ξ_0. 64
4.13 Order parameter versus inverse coherence length $1/\xi_0$. 65
4.14 Temperature dependence of the d-wave OP in the absence of disorder. 66
4.15 Temperature dependence of the d-wave OP for various values of impurity concentration. 66
4.16 Dependence of the critical temperature on the Zn concentration in the Y-Ba-Cu-O compounds. 68
4.17 Dependence of the critical temperature on the Zn concentration in the La-Sr-Cu-O compounds. 68
4.18 The T_c suppression for different potentials. 70
4.19 Dependence of the T_c on the impurity scattering rate for Born and unitary limits. 70
4.20 Calculated influence of Zn impurities on T_c. 71
4.21 Dependence of the order parameter on the impurity concentration in the s-wave superconductors. 72
4.22 Dependence of the order parameter on the impurity concentration in the d-wave superconductors [$\xi_0 \approx 2.5a$]. 73
4.23 Dependence of the order parameter on the impurity concentration in the d-wave superconductors [$\xi_0 \approx 4a$]. 73
4.24 Dependence of the order parameter on the impurity concentration for different values of impurity potentials in the d-wave superconductors [$\xi_0 \approx 4.5a$]. 74
4.25 Dependence of the order parameter on the impurity concentration in the s+d-wave superconductors. 75

List of Tables

2.1 Some characteristics of high-T_c oxide superconductors. 8

2.3 Typical parameters of the high-T_c oxide superconductors. 12

2.4 The electronic configurations of the elements in the YBCO cuprates. 16

2.5 The electronic configurations and ionic radii of some of 3d metal ions and copper. 24

4.1 The critical impurity concentration in the various experiments. . . 69

Chapter 1

INTRODUCTION

Superconductivity is perhaps
the most remarkable
physical property
in the universe.
David Pines

1.1 Low-Temperature Superconductors

Superconductivity was discovered in 1911 by Kamerlingh Onnes. He found that the resistance of a rod of frozen Hg dropped to zero when cooled to the temperature of liquid He (about $4K$). Many other elements, alloys and intermetallic compounds become superconducting when cooled to sufficiently low temperatures. Over the years, the highest transition temperature had been gradually increased from the $4K$ of Hg to $23K$ in the compound Nb_3Ge. In 1950, it was shown that the transition temperature of the superconducting state depends on the isotopic mass of the atoms that make up the metal.[1] This suggests that superconductivity involves an interaction between the conduction electrons and the vibrational motion of the ions in the metal. With this clue, in 1957, microscopic theory[3] (BCS theory) of superconductivity was developed by John Bardeen, Leon N. Cooper, and J. Robert Schrieffer, for which they

were awarded the Nobel Prize in Physics in 1972. This theory was very successful not only in explaining what was known about superconductivity but in predicting a new phenomena, *pairing of electrons*,[4] that later was confirmed by experiments.[5,6] This theory is based on a coherent pairing of electrons where all pairs have identically the same momentum. The pairing results from an attractive interaction between electrons due to coupling to phonons which are quantized modes of atomic vibration that propagate throughout the lattice of a solid. In low-temperature superconductors, quasiparticles (electrons plus their associated screening clouds) disturb the phonons and create a force that overcomes the electrons' repulsive force. The electrons then form a quantum state made up of *Cooper pairs*, which cannot be scattered off by phonons, thereby eliminating resistance. Superconductors exhibit many interesting properties, such as zero resistance and perfect diamagnetism, i. e. the complete expulsion of the magnetic field from the volume of the superconducting sample.

Low temperature superconductors are used in many areas including SQUIDs (Superconducting Quantum Interference Devices), which are capable of detecting minute magnetic fields and electro-magnets, such as those in magnetic resonance imaging devices.

For a general review of low temperature superconductors, see Refs. 7--14.

1.2 High-Temperature Superconductors

One of the greatest events in physics in recent decades was the discovery of high-temperature superconductors, whose resistance become zero at temperatures above $100K$. This new exciting stage began in 1986 when the first high-temperature superconductor was discovered[1] by K. Alex Müller and J. George Bednorz[15] at the IBM Research Laboratory in Zürich, Switzerland. This ceramic compound of lanthanum, barium, copper, and oxygen (LaBaCuO) was becoming

[1]The article, cautiously titled " The possibility of the High-Temperature Superconductivity in the La-Ba-Cu-O system", was turned down by the leading American journal Physical Review Letters.

a superconductor at $35K$. Another team soon found superconductivity in a related material, an yttrium-barium-copper-oxygen compound (YBaCuO), at $90K$, well above the temperature at which nitrogen liquefies (77 K). This is very important, because liquid nitrogen is 50 times cheaper than helium and it promises commercial viability for the new materials. A clear indication of the importance attached to the discovery of these new superconducting materials is that Müller and Bednorz were awarded the Nobel Prize in Physics within a year, 1987.

These new oxide superconductors exhibit the two characteristic properties of conventional superconductors, namely zero resistivity and perfect diamagnetism. In addition to these, they show strong anisotropy in many of their physical properties and they have very short coherence length, large critical temperature, very high critical fields, and a granular composition.

Despite the intensive efforts of the theoretical physics community and thousands of research papers, there is still no clear consensus on the answers to several fundamental questions about the new superconductors. What is the nature of the normal state? What is the character of the superconducting state? What is the physical origin of their superconductivity? What is the symmetry of pairing, i.e. symmetry of order parameter?

Understanding the mechanism responsible for superconductivity in the high-temperature cuprates has been one of the major goals of physicists since the discovery of these exciting materials. Experiments suggest that the pairing state may be unconventional, featuring anisotropic order parameter. What is meant by unconventional superconductors is an order parameter that has a symmetry in momentum space different from the isotropic s-wave Cooper pair, believed to describe all low-temperature superconductors. Many experiments provide strong evidence for existence of nodes with different symmetries. The most serious candidates for the order parameter symmetry, seem to be d-wave or anisotropic s-wave. Beside these many other possible symmetries such as p, d+s and s+id have been proposed. The unconventional pairing differs markedly from the conventional s-wave pairing for which the corresponding energy gap is finite

and almost isotropic.

High-temperature superconductors may have many potential applications in the future. However, many significant material science problems, such as having low current densities and being very brittle and inflexible, must be overcome before such applications become a reality. Assuming that such problems are solved, the possible important applications are

- ➤ low-loss electrical power transmission,
- ➤ the Josephson junction based computer elements,
- ➤ interconnection of computer chips by superconducting wires,
- ➤ high-speed levitated vehicles,
- ➤ construction of high-field superconducting magnets,
- ➤ small-scale superconducting motors,
- ➤ magnetic resonance imaging.

For a general review of high-T_c superconductors, see Refs. 9–12,16–21.

1.3 Motivations and Outline

In Chapter 1 a brief review of high-T_c superconductors will be given, including, crystallographic structures, general properties of normal and superconducting states, pairing mechanism, symmetry of the order parameter, some experiments and impurity effects.

It is well known that nonmagnetic impurities with small concentrations affect neither the transition temperature nor the density of state of BCS superconductors with an isotropic order parameter.[22,89] On the other hand, if the order parameter is anisotropic, then impurity effects become important.[93,95] In Chapter 2 the effects of impurities on isotropic and anisotropic superconductors

will be investigated. A powerful method that uses Bogoliubov-de Gennes equations, will also be studied.

Theoretical calculations and experiments point to many different pairing symmetries such as s, extended s, p, d, s+d and s+id. However, up to now there is no consensus on the symmetry of the order parameters. On the other hand, the effects of nonmagnetic impurities on the properties of superconductors can provide useful information about its order parameter symmetry. Many people[26] think that understanding the impurity effects on high-T_c materials has very crucial role to get information about the underlining mechanism in these materials. Besides this, there are some experimental results which are not completely explained yet, including

❶ rapid suppression of the critical temperature in the presence of some rare earth elements substitutions,

❷ the critical impurity concentration, at which superconductivity vanishes, is smaller in Zn substitution than Ni,

❸ disorder induced by irradiation is always less effective on the critical temperature than the substitutional disorder.

Considering the above arguments, in Chapter 4 Bogoliubov-de Gennes equations are solved on a two-dimensional square lattice to investigate effects of nonmagnetic impurities in high-temperature oxide superconductors. In particular

① possibilities to extract the symmetry of order parameter from the disorder effects will be discussed,

② rapid suppression of the critical temperature of the high-T_c cuprates by substituting the 3d metal ions will be investigated,

③ differences between Zn and Ni substitutions will be explained,

④ considering a-b plane anisotropy, possibility of the admixture of s- and d-wave and its consequences will be discussed.

In the last chapter, the results of the calculations are discussed. Beside this, the results are compared with the experimental observations.

Chapter 2

PROPERTIES OF HIGH-TEMPERATURE OXIDE SUPERCONDUCTORS

In this chapter, a brief review of the high-T_c cuprate[1] compounds in both normal and superconducting phases is given. For this purpose, high-T_c materials can be classified into three classes. Table 2.1 shows some characteristics of these materials. The first class is the one that Bednorz and Müller[15] found. These materials, with the general formula La$\mathcal{M}$CuO ($\mathcal{M}$=Sr, Ba or Ca), contain lanthanum (La), barium (Ba), copper (Cu) and oxygen (O) and exhibit a critical temperature between 30 and $40K$. The second class,so called 1-2-3 compound, were discovered by M. K. Wu and his co-workers.[23] The critical temperature is around $90K$. They contain yttrium (Y), a rare earth element, rather than lanthanum and their general form was YBaCuO. The third class of materials is the one with the highest critical temperature achieved ($125K$) and these materials do not contain rare earth elements. One is a compound of bismuth (Bi), strontium (Sr), calcium (Ca), copper and oxygen (BiSrCuO)[24] while another has thallium

[1]Cuprate means any member of the family of materials having planes of CuO_2 as its building blocks. Most of the high-T_c superconductors are cuprates, but there are other materials like Nb_3Ge and the fullerenes K_3C_{60} which exhibit high-T_c superconductivity.

(Tl) in it instead of bismuth, and barium instead of strontium (TlCaBaCuO).[25]

Compound	Symb	Symm	a_0 (Å)	c_0 (Å)	$T_c(K)$	n(cm^{-3})	Lattice Type
La_2CuO_4 (Sr doped)	0201	O	5.600	13.18	35	$1.5\ 10^{21}$	Perovskites
$YBa_2Cu_3O_7$	0123	O	3.855	11.68	92	$3\ 10^{21}$	layers + chains
$Bi_2Sr_2CaCu_2O_8$	2212	T	5.388	30.60	100	$\sim 10^{21}$	layers
$Tl_2Ba_2Ca_2Cu_3O_{10}$	2223	T	3.850	35.88	125	$\sim 10^{21}$	layers

Table 2.1: Some characteristics of oxide superconductors, Symb ≡ symbol, Symm ≡ symmetry (Orthorhombic O, Tetragonal T), a_0 and c_0 are the lattice parameters, T_c is the transition temperature and n is the carrier density. Taken (modified) from Ref. 10.

In the following sections, properties of the second class (e. g. YBCuO) compounds will be explained.

For a more general review on this topic, see Refs. 17,18,28,29.

2.1 Normal State Properties

The normal state of the cuprate compounds has very unusual properties[2] [See Refs. 30 and 31.]. It is believed that these properties have intrinsic effects on the pairing mechanism in the superconducting phase of these materials. The basic characteristics of the normal state can be summarized as follows (See Table 2.2 for comparison of the normal metal and the normal state of LaSrCuO compound.):

- The dc resistivity ρ depends on the temperature linearly. As shown from Fig. 2.1, as well as linearity, the resistivity is large (poor metal) and highly anisotropic, namely c-axis resistivity is considerably larger than the ab-plane resistivity and in the orthorhombic materials along the plane axes have also different resistivity ($\rho_a \neq \rho_b$).
- The Hall coefficient R_H increases with decreasing temperature (See Fig. 2.2) and this dependence contradicts with the Fermi-liquid theory.

[2]These properties can not be explained in terms of conventional the Fermi-liquid theory.

Quantity	Conventional metal	$La_{1.8}Sr_{0.2}CuO_4$
m^*	[1-15] m_e	5 m_e
k_F [cm^{-1}]	10^8	3.5 x 10^7
v_F [cm/s]	[1-2] 10^8	8 x 10^6
E_F [eV]	5-10	0.1

Table 2.2: Comparison of some parameters of normal metal and normal state of $La_{1.8}Sr_{0.2}CuO_4$ compound. Taken from Ref. 21.

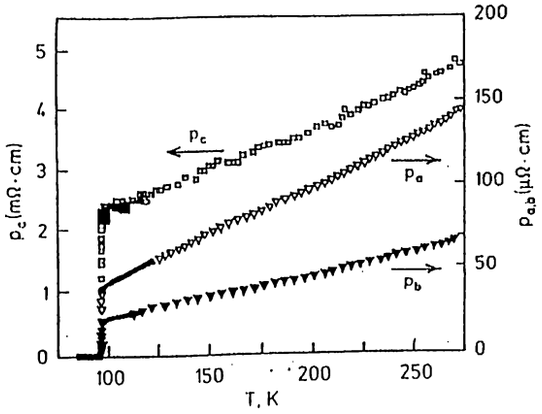

Figure 2.1: Temperature dependence of the resistivity ρ along the three axes of orthorhombic crystals of YBCO. Taken from Ref. 60.

- Fermi energy is almost two orders of magnitude smaller than that of a normal metal. Smallness of this quantity has intrinsic effects on the features of the cuprates.

- The normal state of high-T_c cuprates has an antiferromagnetic ordering (AFM) of the copper spins in the CuO_2 planes. The strong super-exchange interaction between these spins, via oxygen ions, gives rise to a long-range antiferromagnetic order. Although, the long-range AFM ordering disappears in the metallic and the superconducting phases, strong spin fluctuations are observed.

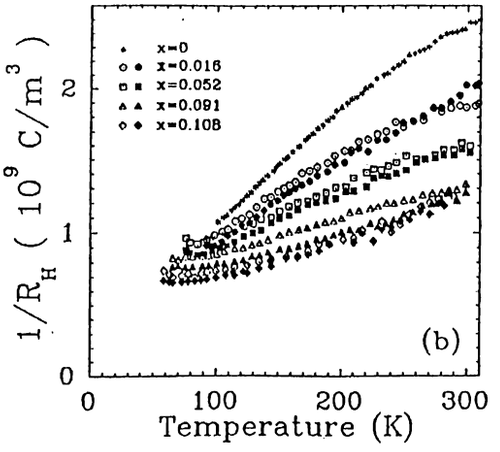

Figure 2.2: Temperature dependence of the inverse Hall coefficient $1/R_H$ for $YBa_2Cu_{3-x}Zn_xO_{7-\delta}$ crystal doped with Zn. Taken from Ref. 61.

2.2 General Properties of Superconducting Phase

It is well known that the oxide superconductors possess many properties in common with conventional superconductors;

- Observation of the usual ac Josephson effect with typical frequency[44] $\omega = 2eV/h$ and the direct measurement of the flux quantum[45] $\phi_0 = hc/2e$ indicates the existence of Cooper pairs with charge $2e$ and zero net momentum (by Andreev's reflection experiment[46]) in the superconducting state.

- The decrease in the Knight shift in the superconducting phase and the temperature dependence of the penetration depth, point to the singlet nature of paring in the usual BCS picture.[32,33]

- In the presence of magnetic fields, flux lattice is observed.

- Tunneling experiments unambiguously indicate the formation of a gap in the spectrum, which also confirms the picture of Cooper pairs.[47]

- Andreev's reflection along time-reversed trajectories is seen.[48]

On the other hand, the high-T_c superconductors have a number of properties different from those of the conventional superconductors, namely

- In the copper-oxide superconductors, the main role is played by CuO_2 planes. Current belief is that superconductivity is confined into these planes which are separated by layers of other ions. Therefore, a high anisotropy of the electronic and superconducting properties, which are of a quasi-two-dimensional character, is specific to the high-T_c oxide materials. The physical properties of the oxide compounds are strongly influenced by the deficiency of oxygen and certain variations in their composition.

- High-T_c cuprate compounds have antiferromagnetic ordering of spins. They are almost localized at Cu sites. Doping CuO_2 planes with charge carriers by variation of the composition, easily destroys the long-range antiferromagnetic order in the metallic state. However, strong dynamical short-range antiferromagnetic fluctuations still exist. The NMR and inelastic neutron scattering experiments confirm the existence of the strong dynamical antiferromagnetic fluctuations. These fluctuations affect the properties of the CuO compounds in the normal phase and may be the origin of non-phononic mechanism of high-T_c superconductors.

- In conventional superconductors, existence of the electron-phonon interaction which is responsible for the pairing mechanism, is confirmed by the large value of the isotope effect exponent, i.e. the critical temperature T_c depends on the mass of the lattice ion ($T_c \propto M^{-\alpha}$, $\alpha \simeq 0.5$). In cuprate compounds this exponent is small in comparison to the conventional superconductors ($\alpha \simeq [0.4 - 0.02]$).[10]

➤ A considerable anisotropy of the gap and a large value of the ratio $2\Delta(0)/kT_c \simeq 3 - 8$[10,17,95] in the planes are specific for layered high-temperature cuprates. This fact clearly distinguishes them from the conventional superconductors, where the gap is rather isotropic and the ratio has the BCS universal value $2\Delta(0)/kT_c \simeq 3.53$.

➤ The coherence length ξ_0 is very small, several lattice constants in the plane while in the direction perpendicular to the plane it is approximately equal to or smaller than the lattice constant. In conventional superconductors $\xi_0 \simeq 10^3 - 10^4$ Å. The smallness of the coherence length,

① indicates that the spatial stretching of the wave function of the Cooper pair points toward a strong coupling of quasi-particles in a pair (such a coupling results in high critical temperature).

② is mainly due to small value of the Fermi velocity[3] (See Table 2.2.),

③ shows that the number of electrons (holes) in the Cooper pairs is smaller by several orders of magnitude than that in conventional superconductors.

For some important implications of short coherence length, see Ref. 138.

➤ The ratio Δ/E_F is very large[4] ($\sim 10^{-1}$) relative to its value in the conventional superconductors ($\sim 10^{-4}$). This ratio is important, because it estimates what fraction of the carriers are directly involved in the pairing. Hence, large value of Δ/E_F means that a significant fraction of the carriers are paired. Of course, this correspond to a short average distance between the paired carriers. As a result of this, the coherence length becomes small. Having large value of Δ/E_F and short coherence length ξ_0 is due to the quasi-2D structure of the cuprates. In the BCS theory ($\Delta/E_F \ll 1$), pairing can occur only near the Fermi surface. On the other hand, the layered structure of the high-T_c oxide superconductors the pairing is possible even for states distant from the Fermi level.

[3] In BCS theory, they are related by $\xi_0 = \hbar v_F/\pi\Delta$.

[4] Small Fermi energy along with large value of the gap.

See Table 2.3 for typical parameters of the high-T_c oxide superconductors.

Quantity	Max value	Min value	Comments
T_c [K]	133	30	for electron SC T_c=[11-22] K
ξ_{ab} [Å]	80	10	
ξ_c [Å]	15	0.2	
λ_{ab} [Å]	2800	260	
λ_c [Å]	35000	1000	
m_c/m_{ab}	730	10	
ρ_0 [$\mu\Omega$cm]	320	0	most frequently [100]
N(E_F) [states/eV]	2.1	0.8	
θ_D [K]	410	250	
Δ_0 [meV]	53	7.4	
$2\Delta_0/k_BT_c$	8	3.1	
$\tilde{\lambda}$	2.0	0.1	
α	0.4	0.02	

Table 2.3: Typical parameters of the high-T_c oxide superconductors. T_c is critical temperature, ξ is coherence length, λ is penetration depth, m_c/m_{ab} is mass ratio, ρ_0 is residual resistivity, N(E_F) is density of states at Fermi level, θ_D is Debye temperature, Δ_0 is energy gap, $2\Delta_0/k_BT_c$ is BCS ratio, $\tilde{\lambda}$ is electron-phonon coupling constant and α is isotope effect exponent. Taken from (modified) Ref. 42. This reference contains an extensive survey of experimental properties of superconductors.

2.3 Structure of the Cuprates

As it is known from crystallographic analysis, high-T_c oxide superconductors are formed on the basis of perovskite-like structures (see Fig. 2.3). The unit cell is made up of one or a few planes of CuO_2 atoms on top of which there are layers of other atoms (Ba, La, Y, ...). This unit cell repeats itself along the z-direction (see Fig. 2.4). As a result of this type of structures, these materials show strong anisotropy in many of their properties. For example, electrical resistivity has very different values when measured parallel to the oxygen-copper planes than

that when measured perpendicular to them (see Fig. 2.1).

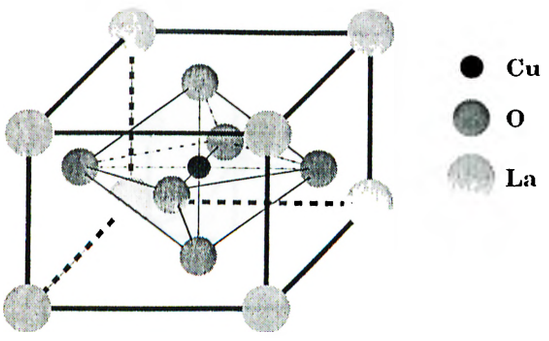

Figure 2.3: The fundamental perovskite unit in the oxide superconductors. As an example $LaCuO_3$ is shown.

The CuO_2 planes are responsible for the superconductivity while the surrounding layers of other atoms provide carriers, electrons or holes. For this reason, the layers neighboring the CuO_2 planes are called the charge reservoirs. The assumption that superconductivity in the high-T_c cuprates is a two-dimensional phenomenon is based on the fact that the distance between CuO_2 planes (≈ 12Å) is larger than Cu-O interspacing (≈ 2Å) so that the electrons (or holes) shared by these atoms are more likely to hoppe within these planes rather than off the planes ($t_{\parallel} \gg t_{\perp}$). The charge is transfered from the reservoir to the conducting planes, when material is doped. Doping means the substitution of atoms in the charge reservoir by others in a different ionization state. As a result, electrons are taken out of the CuO_2 planes or are donated to them. In the former case the carriers of the superconductor current are holes (as in YBCO) while they are electrons (as in BaPbO) in the latter. Carrier type is detected by determining the sign of the Hall coefficient R_H. Also varying the chemical composition of the charge reservoirs, it is possible to change the charge density of the carriers in the CuO_2 planes.

Figure. 2.5 shows schematic lattice structure of the YBCO materials.

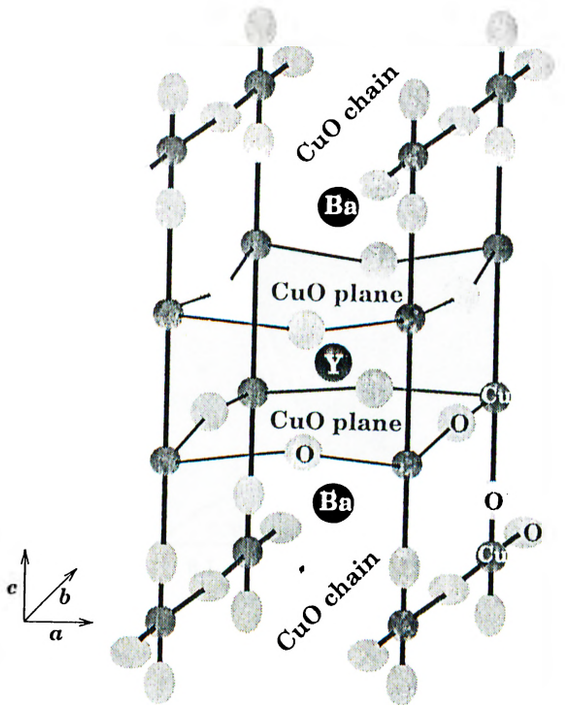

Figure 2.4: Sketch of the superconducting orthorhombic YBaCuO unit cell. It is seen that three planes containing Cu and O are sandwiched between two planes containing Ba and O and one plane containing Y.

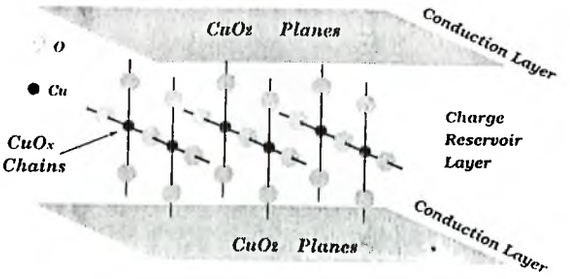

Figure 2.5: Schematic lattice structure of the YBCO compounds.

Phase Diagram

The phase diagram provides useful information about possible mechanism that governs the physics of the cuprates. The main features of the diagram are shown

in Fig. 2.6. Indeed, all oxide cuprates have similar phase diagrams.

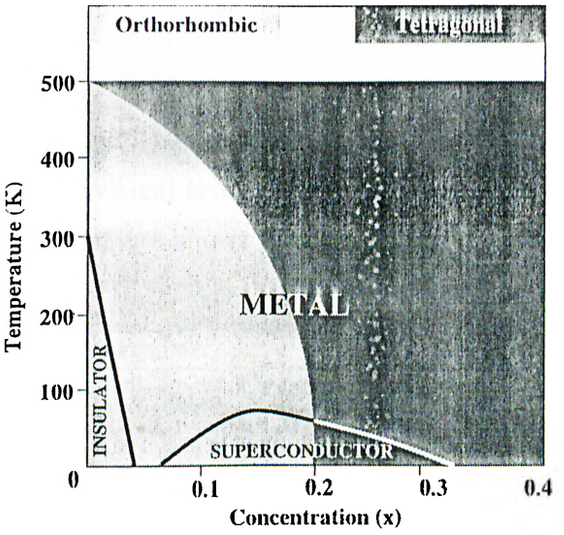

Figure 2.6: Phase diagram of a cuprate compound ($La_{2-x}Sr_xCuO_4$) as a function of temperature.

- If doping is very low ($x \sim 0$), then the material is in antiferromagnetic ordered state with small quantum fluctuations. In this state, the material is an insulator unless the temperature is very high[5].
- With increasing the doping at low temperatures, the material becomes superconductor. When $x \sim 0.15$ (optimal doping), the highest critical temperature is obtained. Further increase in doping above the optimal value causes the critical temperature to decrease.
- When the temperature is above the critical value $T > T_c$, the material is in the normal metallic state. However, as discussed in the previous section, in this state the material may exhibit quite unusual normal state properties.

[5]At high temperature, thermal fluctuations destroy the magnetic order and the material becomes conductor.

2.3.1 Structure of $YBa_2Cu_3O_{6+x}$

In this section a more detailed explanation of properties features of YBCO compounds is given.

Table 2.4 shows the electronic configurations of the elements of YBaCuO. The phase diagram of a YBCO material is drawn in Fig. 2.7. The dependence of lattice parameters, the critical temperature and the effective valence in CuO_2 plane on the oxygen content are shown in Fig. 2.8.

Electronic Configuration	Effective Valence	
	Crystal ($x = 0$)	Doped($x \neq 0$)
^{29}Cu: $3d^{10}$ $4s$	$_{pl}Cu^{2+}$, $_{ch}Cu^{1+}$	$_{pl}Cu^{2.2+}$, $_{ch}Cu^{2.5+}$
^{8}O: $2s^2$ $2p^6$	O^{2-}	O^{2-}
^{39}Y: $5s^2$ $4d$	Y^{3+}	Y^{3+}
^{56}Ba: $6s^2$	Ba^{2+}	Ba^{2+}

Table 2.4: The electronic configurations of the elements in the YBCO cuprates (pl ≡ plane, ch≡chain).

5

The basic properties of YBCO can be summarized as follows:

- There are two CuO_2 planes per unit cell and they are separated by an Y plane.
- Charge reservoir consists of Ba atoms and CuO chains in the b direction.
- At zero doping level; the oxygen atoms are in the O^{2-} state so that they would achieve a complete p-shell, yttrium (barium) loses three (two) electrons and becomes Y^{3+} (Ba^{2+}). Electrical neutrality forces the Copper to adopt the Cu^{2+} in the plane and Cu^{1+} in the chains:

  $2\ Cu^{2+} + 1\ Cu^{1+} + 1\ Y^{3+} + 2\ Ba^{2+} + 6\ O^{2-} = 0$

  If the copper atom loses one electron, then it completes its d-shell but losing one extra electron causes the creation of a hole in this shell. Therefore,

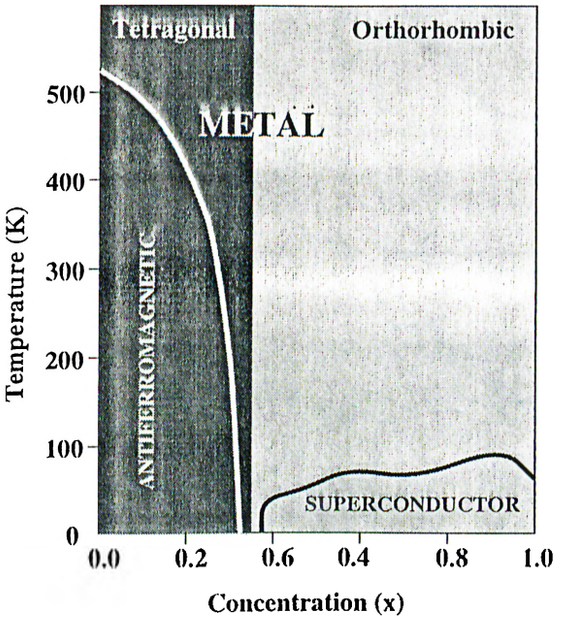

Figure 2.7: Phase diagram of a cuprate compound ($YBa_2Cu_3O_{6+x}$) as a function of temperature.

Cu^{2+} in the planes have a net spin of 1/2. These holes are responsible from the antiferromagnetic long range order observed in the undoped insulating state. Since Cu^{1+} in the chain has net spin zero, it does not contribute to the magnetic effects.

➤ Increasing the doping changes the oxygen content in charge reservoirs and then, since the new oxygens are subtracting electrons from the Cu^{2+} planes, holes are added to the conducting planes.

2.4 Pairing Mechanism

This section deals with the possible origin of pairing mechanism in the high-T_c materials. It is well known that the electron-phonon interactions cause to pairing of electrons in the low-temperature superconductors. Experimental confirmation of large isotope-effect in conventional superconductors gives rise to this

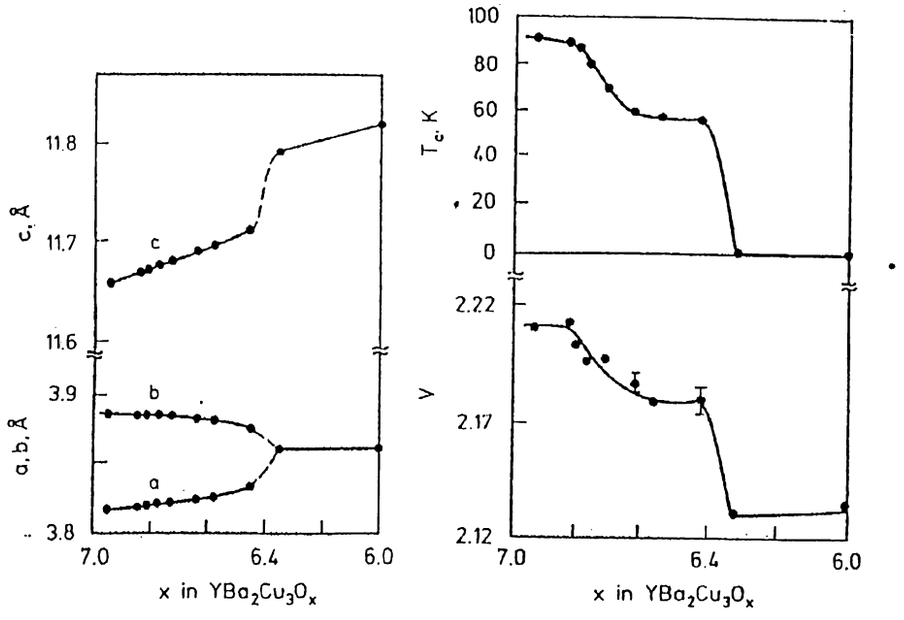

Figure 2.8: Dependence of lattice constants [left panel] , critical temperature and effective valence [right panel] of $YBa_2Cu_3O_x$ on the oxygen content. Taken from Ref.17.

conclusion. However, this is not completely true for high-T_c superconductivity. Theoretical calculations of the electron-phonon interaction in cuprates suggest that phonons alone can not explain the high-T_c superconductivity[6]. As the critical temperature becomes higher, the isotope effect becomes smaller, suggesting an alternate pairing mechanism involving interactions between electrons. Following the above argument the antiferromagnetic spin fluctuations model is proposed.[115,116] The underlining phenomenon in this model is that an electron scattering off a spin fluctuation can cause a perturbation, that in turn might scatter a second electron, hence these fluctuations might pair electrons. This model predicts $d_{x^2-y^2}$ pairing symmetry [see the next section].

Another mechanism was suggested by P. W. Anderson, where in the CuO

[6]Electron-phonon coupling parameter can not give rise to a superconducting transition temperature much higher than 30K. Above this temperature large vibrations of the lattice would disturb the role of the lattice in providing the attraction between two electrons.

planes is a BCS-type pairing occurs. There is Josephson-pair tunneling between the layers. In this case the pairing symmetry is anisotropic s-wave [see the next section].

For general review of this subject, see Refs. 59,58,55.

2.5 Symmetry of the Order Parameter

The symmetry of the superconducting order parameter (OP) of the high-T_c superconductor, which is closely related to the mechanism of superconductivity in the cuprates, is a subject of ongoing research. Although early experiments seemed consistent with a BCS-like s-wave (with $l = 0$) pairing, up to now a growing list of theoretical calculations and experiments suggest that the high-temperature cuprates may exhibit an unconventional OP. The unconventional OP has a symmetry in momentum space different from that of the isotropic s-wave Cooper pair state that is believed to describe all of low-temperature superconductors. The most serious candidates for the order parameter seems to be d-wave or anisotropic s-wave. However, there are many other possibilities, such as p-wave (triplet)[53] and an admixture of s and d-wave[7].

Figure. 2.9 shows the s, extended s and d-wave order parameter symmetries and the corresponding densities of states.

Some experiments and theoretical calculations are in favor of d-wave picture, including

- ➤ linear temperature dependence of the superconducting penetration depth at low temperatures
- ➤ surface impedance measurements,
- ➤ angle-resolved photoemission spectroscopy (ARPES) studies,
- ➤ specific heat data,

[7]Since YBCuO system has orthorhombic structure, an admixture of s and d-wave components is possible[129]

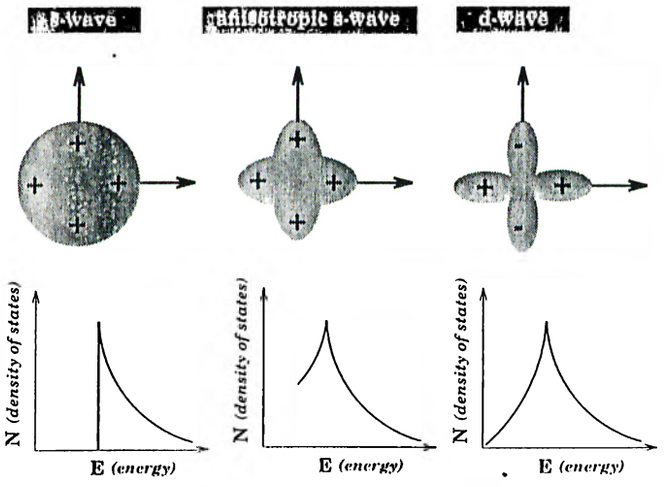

Figure 2.9: Order parameter symmetries and density of states for different pairing symmetries.

- Knight shift,
- nuclear relaxation,
- inelastic neutron scattering,
- Josephson junction experiments in several geometries.

On the other hand, some experiments and theoretical calculations do not support d-wave pairing, including

- c-axis Josephson tunneling measurements,
- grain boundary tunneling studies,
- investigation of nonlinear Meissner effect,
- penetration depth studies on NdCeCuO cuprates,
- neutron scattering.

Some experiments are in favor of s-wave picture, including

- persistent currents and transition temperatures in the composite superconductors consisting of a cuprate and a conventional superconductor (e. g. lead),
- exponentially decreasing surface impedance for a fully oxygenated samples,
- exponential approach of the penetration depth to its zero-temperature value.

It should be noted that the intrinsic complexity of the cuprates has led to contradictory results and confusion in the interpretation of experimental data relevant to the pairing symmetry.

For more extensive discussions, see Refs. 54,59,55–58

Why is identification of the pairing symmetry so important? Firstly, a definitive determination could effectively confirm certain hypotheses about the origin of pairing in the cuprates, e.g. confirmation of the $d_{x^2-y^2}$ pairing is in favor of the antiferromagnetic spin fluctuation mechanism, on the other hand confirmation of the s^+ pairing gives support to phonon mediated mechanism. Secondly, it would have important implications for technology. All high-T_c materials show strong dissipation at low frequencies, even at low temperatures, and this is a major obstacle for efficient device construction. If the pairing has $d_{x^2-y^2}$ symmetry with nodes on Fermi surface, then no refinements will be able to get rid of the low-temperature quasiparticles and resulting dissipation. On the other hand, if the symmetry is s^+, nodeless, then the dissipation may be eliminated by suitable chemical and metallurgical refinements. Another important reason is search for higher T_c by extending the cuprate compounds to three-dimensional structure. An extensive discussion on this topic, can be found in Ref. 27.

2.6 The Effect of Impurity Substitution in the Basal Plane

Among many unusual properties [See section 2.2] of hole-doped high-T_c cuprates, one of the most remarkable is the response of the superconducting state to impurity substitution in the Cu^{2+} basal plane. Contrary to the conventional superconductors, a few percent of diamagnetic (D) [e. g. Zn^{2+}] or appreciably larger amounts of paramagnetic (P) [e. g. Ni^{2+}] materials are enough to suppress the superconductivity completely[8]. At this point, it is important to note that as long as the origin of the pairing in the high-T_c cuprates is due to phonons, effects of D and P impurities are assumed to be equivalent. However, if the pairing is due to antiferromagnetic spin fluctuations, then D impurities have larger effects.[26]

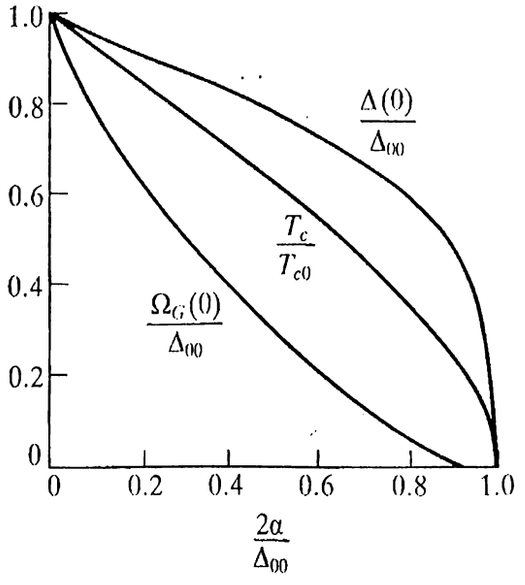

Figure 2.10: The order parameter $\Delta(0)$, critical temperature T_c and energy gap $\Omega(0)$ are plotted as a function of pair breaking parameter α. Δ_{00} and T_{c0} are the corresponding values in the absence of the impurities. Taken from Ref. 90.

[8]For electron-doped superconductors, the situation is similar to BCS superconductors, i. e. D impurities are less effective compared to P impurities. See Ref. 38.

As will be discussed in Chapter 3, in the conventional superconductors, nonmagnetic impurities have no effect on the critical temperature. On the other hand, paramagnetic impurities act as strong pair breakers.[89,90] Hence, they suppress the critical temperature very rapidly. As an example, Fig. 2.10 shows suppression of the order parameter $\Delta(0)$, critical temperature T_c and energy gap $\Omega(0)$ of the low-temperature superconductors in the presence of paramagnetic impurities. In Fig. 2.10, it is important to note that

❶ the pair breaking parameter α is proportional to the concentration of impurities and strength of the impurity potentials.

❷ At some critical concentration, the energy gap vanishes while superconductivity still survives. In this region, the material is called gapless superconductor. The ratio is equal to $n_c(\Omega = 0)/n_c(\Delta = 0) \sim 0.9$. [For very good treatment about gapless superconductivity, see Chapter 10 of Ref.9 and Ref. 34,87.]

❸ The critical temperature changes faster with impurity concentration than the order parameter at zero temperature. Thus the ratio $2\Delta(0,\alpha)/T_c$ is no longer constant, but depends on the impurity concentration.

And also, in Fig. 2.11, the temperature dependence of the order parameter $\Delta(T)$ is plotted for various values of pair breaking parameter α.

Substitution of isovalence 3d metal ions (e. g. $\mathcal{M}$=Zn^{2+}, Ni^{2+}, Fe^{2+},...)[See Table 2.5] instead of copper has a much stronger effect on the critical temperature. In $L\mathcal{M}CO$, superconductivity vanishes at a concentration of $x = 5 - 7\%$ for Ni, Fe, and at $x = 2 - 3\%$ for Zn ions. Figure 2.12 shows dependence of T_c on the Zn impurity concentration x in LSCO and YBCO compounds. The $\mathcal{M}$ ions can behave as magnetic scatterers. Because, they substitute Cu^{2+} ions which have local magnetic moments[9].

In the YBCO compounds, the effect of impurities which substitute for copper ions, is more complicated than in $L\mathcal{M}CO$ compounds, namely

① In YBCO, there are two nonequivalent copper positions, in the planes or along the chains (See Fig. 2.4). Hence, substitution of impurities in the

[9]However, these magnetic moments in the high-T_c materials are not very large to lead to a rapid suppression.

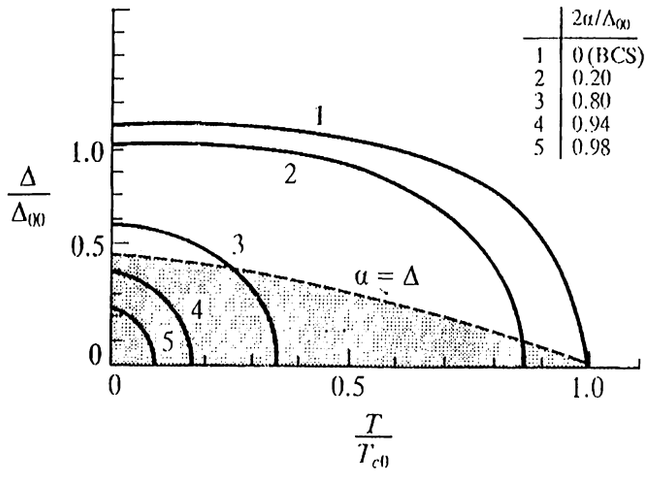

Figure 2.11: The order parameter $\Delta(T)$ versus temperature for several values of pair breaking parameter α. Taken from Ref. 90.

Elements	Electronic Configuration	Ionic Radii r [Å]
$^{26}Fe^{2+}$	$3d^6$	x
$^{27}Co^{2+}$	$3d^7$	x
$^{28}Ni^{2+}$	$3d^8$	x
$^{29}Cu^{2+}$	$3d^9$	0.73
$^{30}Zn^{2+}$	$3d^{10}$	0.75
$^{31}Ga^{3+}$	$3d^{10}$	0.62

Table 2.5: The electronic configurations and ionic radii of some of 3d metal ions and copper. Taken from Refs.43.

different copper positions leads to different effects on electronic structure and superconductivity.

Xiao and his co-workers[43] have studied effects of the chain on the superconductivity. They have concluded that existence of the Cu-O chain structure is insignificant to the high-T_c superconductivity. Figure 2.13 displays lattice parameters and the critical temperature of the YBCO compounds as a

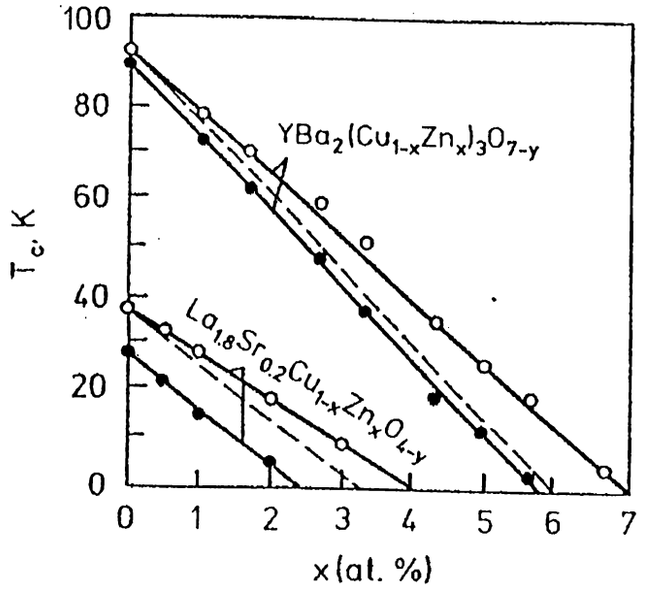

Figure 2.12: Dependence of the T_c on the Zn concentration in $La_{1.8}Sr_{0.2}Cu_{1-x}Zn_xO_4$ and $YBa_2(Cu_{1-x}Zn_x)_3O_{7-y}$. The T_c is measured with respect to the change of the resistance $R(T)$ slope is shown by open circles, and $T_c(R=0)$ by filled circles. Taken from Ref. 17.

function of Zn and Ga concentrations. As shown in the top-right panel of the Fig. 2.13, small doping of the Ga induces an orthorhombic-to-tetragonal structural transition. On the contrary, Zn doping retains the initial orthorhombic structure. The Zn ions suppress the superconductivity very effectively and the superconductivity completely vanishes at 12-13 % of Zn (See bottom-left panel of the Fig. 2.13). On the Other hand, Ga initially decreases T_c at a rate 1K per % Ga concentration, after 6 % T_c does not decrease any more (See bottom-right panel of the Fig. 2.13).

The Neutron diffraction experiments demonstrate that Zn and Ga preferentially occupy Cu-site in the plane[10] and in the chain, respectively. These studies lead to the conclusion that most important feature in the high-T_c superconductors is the CuO_2 planes, while the role of the the chain is rather minor. This conclusion

[10]At the larger concentration, the Zn ions start to occupy Cu-site in the chain.

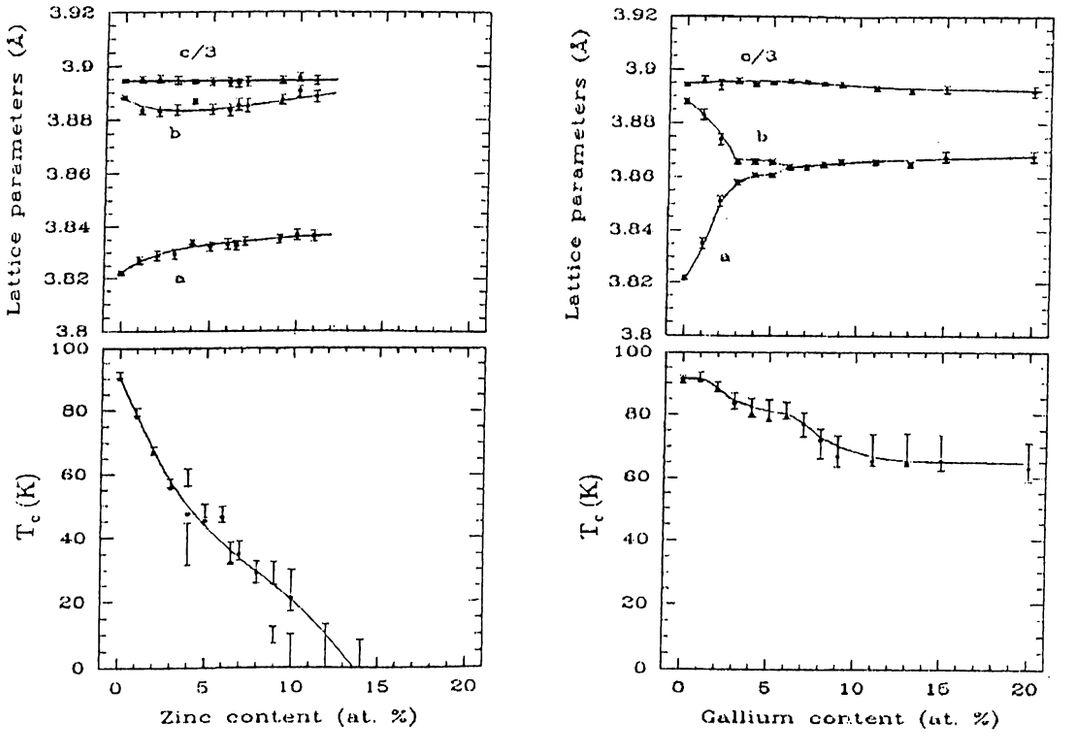

Figure 2.13: (a) Lattice parameter of $YBa_2(Cu_{1-x}\mathcal{M}_x)_3O_{7-y}$ as a function of Zn content [top-left panel] and Ga content [top-right panel] . (b) Variation of T_c with x. Taken from Ref. 43.

is tested by doping the same ions in chain free LaSrCuO compounds. The value of T_c is found to be severely affected by both Zn and Ga ions.

② Some impurities, e. g. Zn, preserve the orthorhombic phase, while others lead to a transition to the tetragonal phase (See Fig. 2.14 [left panel]).

③ Some impurities, e. g. Co and Fe, affect the oxygen content and the short-ranged order in the CuO chain, which may change the number of carriers in the CO_2 planes (See Fig. 2.14 [right panel]).

Figure. 2.15 shows suppression of the critical temperature of YBCO materials as a function of the dopant concentration for several isovalence 3d metal ions. It should be noted that in a serious of experiments, very different (and complicated) T_c dependence on the concentration of impurities, which substitute in Cu-site in

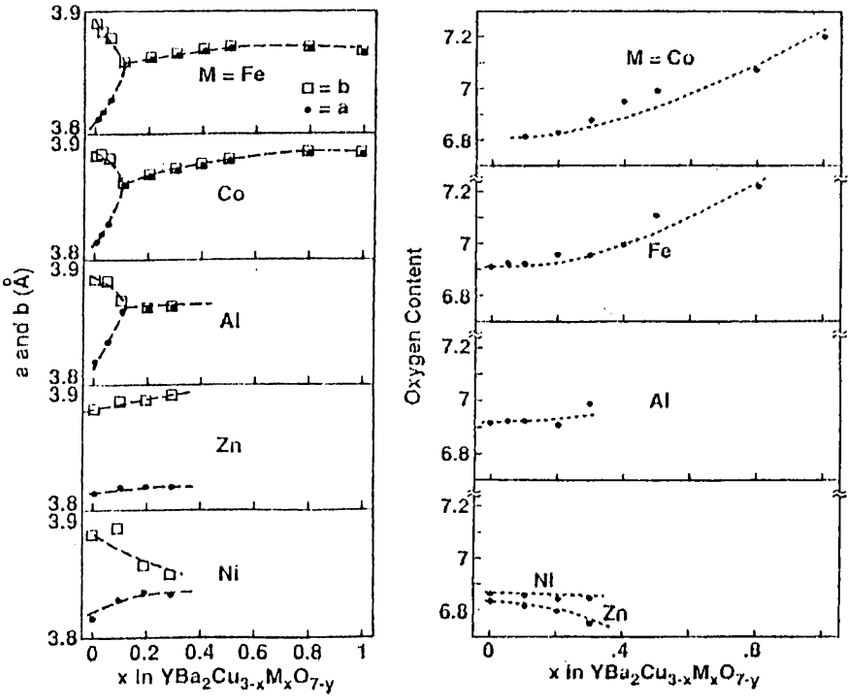

Figure 2.14: The variation of the lattice parameters a and b [left panel] and the oxygen content [right panel] of $YBa_2Cu_{3-x}\mathcal{M}_xO_{7-y}$ as a function of x. Taken from Ref. 40.

YBCO materials, has been observed. Probably, the discrepancy in the data for $T_c(x)$ is related to

❶ insufficient control of the actual impurity concentration,

❷ solubility of impurity ions in the samples,

❸ complexity of the high-T_c cuprate materials (i. e. containing boundaries, defects, ...).

For more extensive studies on the impurity effects, see Refs.17,34–41.

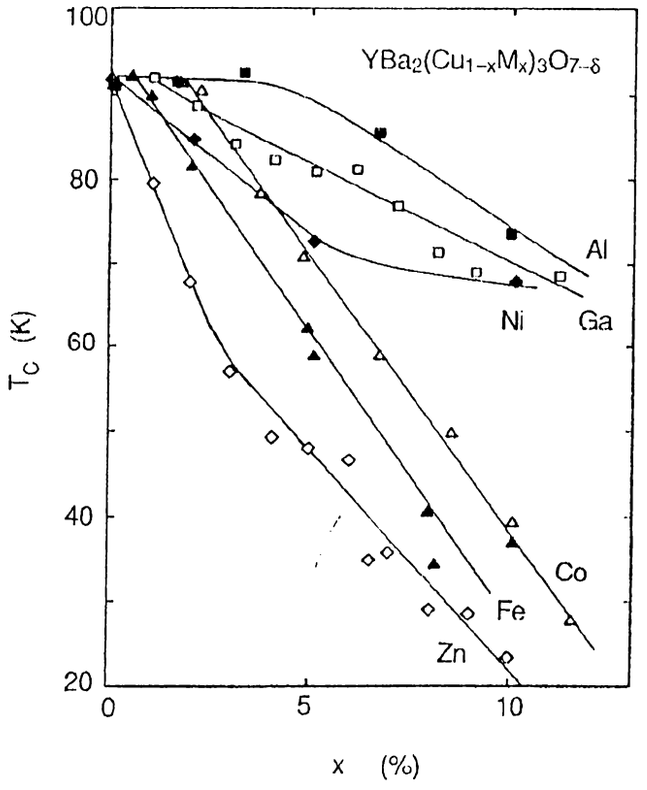

Figure 2.15: The critical temperature T_c versus dopant concentration x for $YBa_2Cu_{3-x}\mathcal{M}_xO_{7-\delta}$. Taken from Ref. 39.

2.7 Review of Experiments

In this section, a brief review of a few experiments is given. These experiments are used to study impurity effects on high-T_c cuprate superconductors. For more extensive discussions of the experiments, see Refs. 62,10.

❑ Muon Spin Rotation (μSR)

The muon[11] spin rotation (μSR) method is a unique tool for investigating the local magnetic field distribution in a superconductor. By using this

[11]The positive muon μ^+ is a lepton with a mass of $m_\mu \simeq 207 m_e$ (m_e is electron mass) and spin $s = 1/2$.

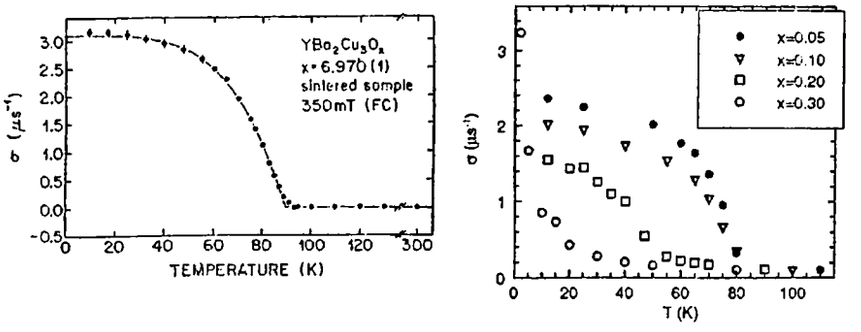

Figure 2.16: Temperature dependence of the depolarization rate σ for $YBa_2Cu_3O_x$ [left panel] and $Y(Ba_{1-x}La_x)_2Cu_3O_7$ [right panel]. Taken from Refs. 49 and 50.

technique, various magnetic properties, such as Meissner effect, diamagnetic shielding, vortex structure, penetration depth of the oxide superconductors, can be determined. If the pairing mechanism in the cuprate compounds is due to magnetism, then the results of μSR experiments play crucial role in understanding the origin of pairing.

In these experiments, the muon-spin depolarization (damping) rate σ is measured. This quantity provides information on the average local field distribution $< \Delta B_\mu^2 > \propto \sigma^2$ in the sample.

As an example, Fig. 2.16 shows depolarization rate σ as a function of temperature for $YBa_2Cu_3O_x$ [left panel] and $Y(Ba_{1-x}La_x)_2Cu_3O_7$ [right panel] compounds.

For a complete review of this method, see.[49,51,52]

❑ Nuclear Magnetic Resonance (NMR)

NMR involves the interaction of a nucleus possessing a nonzero spin I with an applied magnetic field B_0 giving the energy level

$$E_m = \gamma \hbar B_0 m \qquad\qquad m = -I...I$$

NMR studies probe the local magnetic field around an atom and hence reflect the susceptibility of the material. The importance of NMR studies arises from

that it is a unique tool to clarify whether spin correlations play a crucial role in the mechanism of superconductivity or not.

❑ **Inelastic Neutron Scattering**

This experiment enables to us determine the susceptibility as a function of wavevector as well as frequency. It essentially probes the spin excitation processes. Since the scattered neutron interacts with a magnetic moment of transition ions that are present in the sample, the resulting diffraction pattern gives us information about the spin direction.

❑ **Mössbauer Resonance**

Mössbauer resonance measures gamma rays emitted by a recoilless nucleus when it undergoes a transition from a nucleus ground state to a nuclear excited state. This experiment probes the chemical environment of the nucleus in the lattice. The Mössbauer spectra provides us helpful information about the valence state of the nucleus.

Chapter 3

ISOTROPIC AND ANISOTROPIC IMPURE SUPERCONDUCTORS

In this chapter, the Bogoliubov-de Gennes equations and effect of nonmagnetic impurities on the isotropic and anisotropic superconductors are studied.[1]

3.1 The Self-consistent Field Method: Bogoliubov-de Gennes Equations

In this section, a review of the Bogoliubov-de Gennes (BdG) equations, which are essentially a generalization of the Hartree-Fock equations to the case of superconductivity, is given. They have been introduced by Bogoliubov[63,64] and investigated by de Gennes.[8] These equations have been widely used to study disordered superconductors,[65–68] superconducting quantum wells[69] and nanostructures,[70] surface superconductivity,[71] quasiparticle spectrum for d-wave superconductors,[72] vortices in type-II[73–77] and d-wave superconductors[78,79] and twin boundaries.[80,81]

[1] $k_B = 1$ and $\hbar = 1$ are taken throughout this chapter.

Consider an interacting electron gas in the presence of an arbitrary external potential $U_0(\mathbf{r})$ and a magnetic field $\mathbf{B} = \nabla \times \mathbf{A}$. The Hamiltonian of the system can be written in terms of field operators $c_\sigma(\mathbf{r})$ and $c_\sigma^\dagger(\mathbf{r})$ (See Ref. 82 for a review.)

$$\begin{aligned} H = H_0 + H_{int} &= \int d\mathbf{r} \sum_\sigma c_\sigma^\dagger(\mathbf{r}) \left[\left(\mathbf{p} - \frac{e}{c}\mathbf{A} \right)^2 + U_0(\mathbf{r}) \right] c_\sigma(\mathbf{r}) \\ &\quad - \frac{1}{2} \int \int d\mathbf{r}\, d\mathbf{r}' \sum_{\sigma\sigma'} c_\sigma^\dagger(\mathbf{r}) c_{\sigma'}^\dagger(\mathbf{r}')\, V(\mathbf{r},\mathbf{r}')\, c(\mathbf{r}')_{\sigma'} c_\sigma(\mathbf{r}), \quad (3.1) \end{aligned}$$

where the operator $c_\sigma^\dagger(\mathbf{r})$ $[c_\sigma(\mathbf{r})]$ creates [annihilates] an electron with spin σ at position $\mathbf{r}$, $\mathbf{p} = -i\hbar\nabla$ and $U_0(\mathbf{r})$ describes the effects of disorder which does not depend on spin indices[2]. In the preceding equation, the second term describes electron-electron interaction with some approximations:

❶ coupling is spin-independent[3] and

❷ pointlike $V(\mathbf{r},\mathbf{r}') = V\delta(\mathbf{r}-\mathbf{r}')$ and thus characterized by only one coefficient V. Notice that the effect of magnetic field on spins of conduction electron is ignored[4].

Note that the field operators $c_\sigma(\mathbf{r})$ in (3.1) can be expanded by plane wave basis $\phi_\mathbf{k}(\mathbf{r}) = e^{i\mathbf{k}\cdot\mathbf{r}}$, leading to

$$c_\sigma(\mathbf{r}) = \sum_k \phi_\mathbf{k}(\mathbf{r}) a_{\mathbf{k}\sigma}, \quad (3.2)$$

where the operator $a_{\mathbf{k}\sigma}^\dagger$ $[a_{\mathbf{k}\sigma}]$ creates [annihilates] an electron with spin σ and momentum $\mathbf{k}$.

The new operators in (3.2), $c_\sigma^\dagger(\mathbf{r})$ and $c_\sigma(\mathbf{r})$, satisfy the fermionic anticommutation relations

$$\left\{ c_\sigma^\dagger(\mathbf{r}), c_{\sigma'}(\mathbf{r}') \right\} = c_\sigma^\dagger(\mathbf{r}) c_{\sigma'}(\mathbf{r}') + c_{\sigma'}(\mathbf{r}') c_\sigma^\dagger(\mathbf{r}) = \delta(\mathbf{r}-\mathbf{r}')\, \delta_{\sigma,\sigma'}$$

[2]This assumption is correct for only nonmagnetic materials, for magnetic case spin-dependent exchange potential is necessary.

[3]For magnetic media, spin dependency must be taken into account.

[4]This assumption is correct for $\Delta > \omega$, where $\omega = \frac{eB}{mc}$. Here m is electron mass.

$$\begin{aligned}\{c_\sigma(\mathbf{r}), c_{\sigma'}(\mathbf{r}')\} &= 0 \\ \left\{c_\sigma^\dagger(\mathbf{r}), c_{\sigma'}^\dagger(\mathbf{r}')\right\} &= 0. \end{aligned} \tag{3.3}$$

Eq. (3.1) can be solved by replacing the interaction term $Vc_\sigma^\dagger(\mathbf{r})c_{\sigma'}^\dagger(\mathbf{r})c_{\sigma'}(\mathbf{r}')c_\sigma(\mathbf{r})$ by an average potential acting on only one electron at a time, therefore the interaction contains only two operators. Trying an effective Hamiltonian of the form

$$\begin{aligned} H_{eff} &= H_0 \\ &+ \int d\mathbf{r} \left[\sum_\sigma U(\mathbf{r})c_\sigma^\dagger(\mathbf{r})c_\sigma(\mathbf{r}) + \Delta(\mathbf{r})c_\uparrow^\dagger(\mathbf{r})c_\downarrow^\dagger(\mathbf{r}) + \Delta^*(\mathbf{r})c_\downarrow(\mathbf{r})c_\uparrow(\mathbf{r})\right], \end{aligned} \tag{3.4}$$

where $U(\mathbf{r})$ and $\Delta(\mathbf{r})$ are effective potential and pair potential, respectively. They are determined self-consistently. Eq.(3.4) can be diagonalized by performing a unitary transformation, so called Bogoliubov transformation,

$$\begin{aligned} c_\uparrow(\mathbf{r}) &= \sum_n \left(\gamma_{n\uparrow}\, u_n(\mathbf{r}) - \gamma_{n\downarrow}^\dagger\, v_n^*(\mathbf{r})\right) \\ c_\downarrow(\mathbf{r}) &= \sum_n \left(\gamma_{n\downarrow}\, u_n(\mathbf{r}) + \gamma_{n\uparrow}^\dagger\, v_n^*(\mathbf{r})\right), \end{aligned} \tag{3.5}$$

where the γ and $\gamma^\dagger$ are new operators still satisfy the fermionic commutation relations

$$\begin{aligned} \left\{\gamma_{m\sigma}^\dagger, \gamma_{n\sigma'}\right\} &= \gamma_{m\sigma}^\dagger\gamma_{n\sigma'} + \gamma_{n\sigma'}\gamma_{m\sigma}^\dagger = \delta_{mn}\delta_{\sigma\sigma'} \\ \left\{\gamma_{m\sigma}^\dagger, \gamma_{n\sigma'}^\dagger\right\} &= 0 \\ \{\gamma_{m\sigma}, \gamma_{n\sigma'}\} &= 0. \end{aligned} \tag{3.6}$$

After the transformation (3.5), H_{eff} will be diagonalized, that is,

$$H_{eff} = E_0 + \sum_{n\sigma} E_n \gamma_{n\sigma}^\dagger \gamma_{n\sigma}, \tag{3.7}$$

where E_0 is the ground state energy and E_n is the energy of the n^{th} excited state. By taking the commutators of the H_{eff} with $\gamma_{n\sigma}^\dagger$ and $\gamma_{n\sigma}$, the following expressions are obtained:

$$[\gamma_{n\sigma}, H_{eff}] = E_n \gamma_{n\sigma}$$

$$[\gamma^\dagger_{n\sigma}, H_{eff}] = -E_n \gamma^\dagger_{n\sigma}. \tag{3.8}$$

Note that (3.8) fixes the functions u_n and v_n in (3.5). The equations for u_n and v_n can be found from the commutators $[c, H_{eff}]$ and $[c\dagger, H_{eff}]$. By using the definition (3.1) of H_{eff} and the anticommutation properties (3.3) of c and $c\dagger$

$$\begin{aligned} [c_\uparrow(\mathbf{r}), H_{eff}] &= [H_0 + U(\mathbf{r})]\, c_\uparrow(\mathbf{r}) + \Delta(\mathbf{r})\, c^\dagger_\downarrow(\mathbf{r}) \\ \left[c^\dagger_\downarrow(\mathbf{r}), H_{eff}\right] &= -[H_0^* + U(\mathbf{r})]\, c^\dagger_\downarrow(\mathbf{r}) + \Delta^*(\mathbf{r})\, c_\uparrow(\mathbf{r}). \end{aligned} \tag{3.9}$$

In (3.9), the c's can be replaced by the γ's by using (3.5). Finally, by using the commutation relations (3.8) and comparing the coefficients of γ_n (and $\gamma^\dagger_n$) on both sides of the equations, the Bogoliubov-de Gennes (BdG) equations are obtained:

$$\begin{aligned} E_n u_n(\mathbf{r}) &= [H_0 + U(\mathbf{r})]\, u_n(\mathbf{r}) + \Delta(\mathbf{r})\, v_n(\mathbf{r}) \\ E_n v_n(\mathbf{r}) &= -[H_0^* + U(\mathbf{r})]\, v_n(\mathbf{r}) + \Delta^*(\mathbf{r})\, u_n(\mathbf{r}), \end{aligned} \tag{3.10}$$

or in matrix form

$$\begin{pmatrix} H_0 + U(\mathbf{r}) & \Delta(\mathbf{r}) \\ \Delta^*(\mathbf{r} & -[H_0 + U(\mathbf{r})] \end{pmatrix} \begin{pmatrix} u_n(\mathbf{r}) \\ v_n(\mathbf{r}) \end{pmatrix} = E_n \begin{pmatrix} u_n(\mathbf{r}) \\ v_n(\mathbf{r}) \end{pmatrix}. \tag{3.11}$$

Note that if $(u_n\ v_n)$ is a solution with eigenvalue E, then $(-v_n^*\ u_n^*)$ is also a solution with eigenvalue $-E$ and hence it is enough to find solutions with $E > 0$.

Now, it still remains to determine the self-consistency equations for effective potentials $U(\mathbf{r})$ and $\Delta(\mathbf{r})$. Let us introduce the probability of finding a quasiparticle of spin σ [5]

[5] In most cases $f_{n\sigma}$ does not depend on spin indices, therefore it is taken simply f_n.

$$f_{n\sigma} =< \gamma^{\dagger}_{n\sigma}\gamma_{n\sigma} > \tag{3.12}$$

where <> denotes a thermal average. The free energy of the original Hamiltonian (3.1) is

$$\mathcal{F} =< H > -TS, \tag{3.13}$$

where T is temperature and S is the entropy of the system

$$S = -\sum_{n\sigma} f_n \ln f_n - (1 - f_n)\ln(1 - f_n) \tag{3.14}$$

and $< H >$ is the mean value of (3.1), that is,

$$< H >=< H_0 > -\frac{1}{2}V\int d\mathbf{r} \sum_{\sigma\sigma'} < c^{\dagger}_{\sigma}(\mathbf{r})c^{\dagger}_{\sigma'}(\mathbf{r}')c_{\sigma'}(\mathbf{r}')c_{\sigma}(\mathbf{r}) > . \tag{3.15}$$

The product $< c^{\dagger}c^{\dagger}cc >$ can be simplified by using Wick's theorem[83]

$$\begin{aligned} < c^{\dagger}(1)c^{\dagger}(2)c(3)c(4) > \;=\; & < c^{\dagger}(1)c(4) >< c^{\dagger}(2)c(3) > \\ & - < c^{\dagger}(1)c(3) >< c^{\dagger}(2)c(4) > \\ & + < c^{\dagger}(1)c^{\dagger}(2) >< c(3)c(4) > \end{aligned} \tag{3.16}$$

By combining (3.13), (3.15), and (3.16), variation of the free energy is given by

$$\begin{aligned} \delta\mathcal{F} = \delta < H_0 > -\frac{1}{2}V\int d\mathbf{r} \sum_{\sigma\sigma'} \quad & \delta\{ < c^{\dagger}_{\sigma}(\mathbf{r})c_{\sigma}(\mathbf{r}) >< c^{\dagger}_{\sigma'}(\mathbf{r}')c_{\sigma'}(\mathbf{r}') > \\ & - < c^{\dagger}_{\sigma}(\mathbf{r})c_{\sigma'}(\mathbf{r}') >< c^{\dagger}_{\sigma'}(\mathbf{r})c_{\sigma}(\mathbf{r}) > \\ & + < c^{\dagger}_{\sigma}(\mathbf{r})c^{\dagger}_{\sigma'}(\mathbf{r}' >< c_{\sigma}(\mathbf{r})c_{\sigma'}(\mathbf{r}') > \} \\ & -T\delta S. \end{aligned} \tag{3.17}$$

The distribution function, f_n, can be determined by minimizing (3.17) with respect to f_n. The resulting expression is nothing but the Fermi-Dirac distribution

$$f_n = \frac{1}{\exp(E_n/T) + 1}. \tag{3.18}$$

Varying the amplitudes $(u_n\ v_n)$ to $(u_n + \delta u_n, v_n + \delta v_n)$ and f_n to $f_n + \delta f_n$, the free energy (3.17) then varies by $\delta\mathcal{F}$, that is,

$$\begin{aligned}\delta\mathcal{F} = \delta < H_0 > -\frac{1}{2}V\int d\mathbf{r} \sum_{\sigma\sigma'} \quad & \{\ \delta < c^\dagger_\sigma(\mathbf{r})c_\sigma(\mathbf{r}) >< c^\dagger_{\sigma'}(\mathbf{r}')c_{\sigma'}(\mathbf{r}') > \\ & + < c^\dagger_\sigma(\mathbf{r})c_\sigma(\mathbf{r}) > \delta < c^\dagger_{\sigma'}(\mathbf{r}')c_{\sigma'}(\mathbf{r}') > \\ & -\delta < c^\dagger_\sigma(\mathbf{r})c_{\sigma'}(\mathbf{r}') >< c^\dagger_\sigma(\mathbf{r}')c(\mathbf{r})_\sigma > \\ & < c^\dagger_\sigma(\mathbf{r})c_{\sigma'}(\mathbf{r}') > \delta < c^\dagger_\sigma(\mathbf{r}')c(\mathbf{r})_\sigma > \\ & +\delta < c^\dagger_\sigma(\mathbf{r})c^\dagger_{\sigma'}(\mathbf{r}' >< c_\sigma(\mathbf{r})c_{\sigma'}(\mathbf{r}') > \\ & + < c^\dagger_\sigma(\mathbf{r})c^\dagger_{\sigma'}(\mathbf{r}' > \delta < c_\sigma(\mathbf{r})c_{\sigma'}(\mathbf{r}') >\ \} \\ & -T\delta S. \end{aligned} \tag{3.19}$$

Note that the free energy of effective Hamiltonian (3.4)

$$\tilde{\mathcal{F}} =< H_{eff} > -TS \tag{3.20}$$

is stationary with respect to δu_n, δv_n, and δf_n since the excitations diagonalize H_{eff} exactly. By using (3.4), this condition gives

$$\begin{aligned}\delta\tilde{\mathcal{F}} = 0 \ = \ & \delta < H_0 > + \int d\mathbf{r}\left[\sum_\sigma U(\mathbf{r})\ \delta < c^\dagger_\sigma(\mathbf{r})c_\sigma(\mathbf{r}) > + \Delta(\mathbf{r})\ \delta < c^\dagger_\downarrow(\mathbf{r})c^\dagger_\downarrow(\mathbf{r}) > \right. \\ & \left. + \Delta^*(\mathbf{r})\ \delta < c_\downarrow(\mathbf{r})c_\downarrow(\mathbf{r}) >\right]. \end{aligned} \tag{3.21}$$

Comparing (3.19) and (3.21), F will be stationary if the effective and pair potentials are taken to be

$$\begin{aligned} U(\mathbf{r}) \ &= \ V < c^\dagger_\downarrow(\mathbf{r})c_\downarrow(\mathbf{r}) >= V\sum_n \left(|u_n(\mathbf{r})|^2 f_n + |v_n(\mathbf{r})|^2(1-f_n)\right) \\ \Delta(\mathbf{r}) \ &= \ V < c_\downarrow(\mathbf{r})c_\downarrow(\mathbf{r}) >= -V\sum_n u_n(\mathbf{r})v^*_n(\mathbf{r})(1-2f_n). \end{aligned} \tag{3.22}$$

Note that there is an important distinction between U and Δ. U is nearly independent of temperature. On the contrary, the pair potential Δ is a sum of terms of the form $u_n v_n^*$. Such terms are nonzero only in the neighborhood of the Fermi surface. For this reason Δ is a rapidly varying function of temperature.

3.2 Effects of Nonmagnetic Impurities on Isotropic Superconductors

Anderson,[22] and Abrikosov and Gor'kov[84] have shown independently that a small amount of nonmagnetic impurities do not effect the thermodynamic properties of a superconductor, as it has been verified by experiments.[85,86] This fact can be stated in somewhat more general form:

If an external perturbation does not break the time-reversal symmetry and does not cause a long-range spatial variation of order parameter, $\Delta(\mathbf{r}) = \Delta_0 =$ *const.*, the thermodynamic properties of a superconductor remain unchanged in the presence of the perturbation[6]. This theorem can be shown by solving (3.10) without magnetic field, that is,

$$\begin{aligned} E_n u_n(\mathbf{r}) &= \left(-\frac{1}{2m}\nabla^2 + U(\mathbf{r})\right) u_n(\mathbf{r}) + \Delta(\mathbf{r})\, v_n(\mathbf{r}) \\ E_n v_n(\mathbf{r}) &= \left(\frac{1}{2m}\nabla^2 - U(\mathbf{r})\right) v_n(\mathbf{r}) + \Delta^*(\mathbf{r})\, u_n(\mathbf{r}), \end{aligned} \tag{3.23}$$

where $U(\mathbf{r})$ contains the impurity potentials. Let's introduce the one-electron wave functions in the normal state $\psi_n(\mathbf{r})$, which is a solution of

$$\left(-\frac{1}{2m}\nabla^2 + U(\mathbf{r})\right) \psi_n(\mathbf{r}) = \xi_n \psi_n(\mathbf{r}). \tag{3.24}$$

For pure metal ($U(\mathbf{r}) = 0$) the $\psi_n(\mathbf{r})$ are Bloch waves. In the presence of scatterers, the wave functions of electrons are complicated and resulting wave functions

[6] In the presence of magnetic impurities, spin exchange field and magnetic field, time reversal symmetry is broken. As a result, these perturbations are responsible from the pair-breaking mechanism. See Ref. 87 for a more extensive discussion on this topic.

describe the successive scattering of an electron by all of the scatterers. When the pair potential is independent of $\mathbf{r}$, i.e. $\Delta(\mathbf{r}) = \Delta$, even in the presence of disorder [7], it can be assumed that $u_n(\mathbf{r})$ is proportional to the normal state wave function $\psi_n(\mathbf{r})$,[88] that is,

$$\begin{aligned} u_n(\mathbf{r}) &= u_n \psi_n(\mathbf{r}) \\ v_n(\mathbf{r}) &= v_n \psi_n(\mathbf{r}), \end{aligned} \tag{3.25}$$

where u_n, v_n and $\psi_n(\mathbf{r})$ can be chosen to be real. (This is possible because the wave functions $\psi_n(\mathbf{r})$ are eigenfunctions of a real operator.)
Inserting (3.25) into (3.23)

$$\begin{aligned} (E_n - \xi_n)\, u_n - \Delta v_n &= 0 \\ \Delta u_n - (E_n + \xi_n)\, v_n &= 0. \end{aligned} \tag{3.26}$$

From the solution of (3.26), the following equation is obtained

$$E_n = \sqrt{\xi_n^2 + \Delta^2} \tag{3.27}$$

and

$$\begin{aligned} u_n &= \left(\frac{1}{2} + \frac{\xi_n}{2E_n} \right)^{1/2} \\ v_n &= \left(\frac{1}{2} - \frac{\xi_n}{2E_n} \right)^{1/2} \end{aligned} \tag{3.28}$$

The self-consistency equation (3.22) becomes

$$\Delta(\mathbf{r}) = V \sum_n |\psi_n(\mathbf{r})|^2 \frac{\Delta(\mathbf{r})}{2\sqrt{\xi_n^2 + \Delta(\mathbf{r})^2}} \left(1 - 2f\left(\sqrt{\xi_n^2 + \Delta(\mathbf{r})^2} \right) \right). \tag{3.29}$$

[7] This approximation is not correct rigorously, but has been shown to be acceptable if impurity concentration is small and the potentials of the scatterers are not chemically too different from the system.

Introducing the density of states at the Fermi level $N(\mathbf{r})$ at the point $\mathbf{r}$ in the normal metal

$$N(\mathbf{r}) = \sum_{n} |\psi_n(\mathbf{r})|^2 \delta(\xi_n). \tag{3.30}$$

The self-consistency condition (3.29) becomes

$$\Delta(\mathbf{r}) = VN(\mathbf{r}) \int_{-\omega_D}^{\omega_D} \frac{\Delta(1-2f)}{2\sqrt{\xi_n^2 + \Delta^2}}\, d\xi. \tag{3.31}$$

The self-consistency (3.31) cannot be exact since Δ was assumed to be constant, but here $\Delta(\mathbf{r})$ is modified by the scatterers. However, if the potentials of the scatterers are chemically similar to the system, $N(\mathbf{r})$ is not very different from its average $\bar{N}$ and then the self-consistency have the same form as for pure superconductors, so that

$$1 = V\bar{N} \int_{-\omega_D}^{\omega_D} \frac{(1-2f)}{2\sqrt{\xi_n^2 + \Delta^2}}\, d\xi, \tag{3.32}$$

which means that Δ is unaffected by impurities. This conclusion will be also recovered in Chapter 4 by solving BdG numerically for isotropic s-wave.

Since nonmagnetic impurities act only on the electric charge and scatter both electrons of the Cooper pairs identically, the superconductivity is not collapsed. On the other hand, for magnetic impurities these situations are completely different. Magnetic impurities are capable of flipping of the electron spin. Due to this flipping, the pairs can go to a state with parallel spins. In this case, Pauli exclusion principle requires that electrons in the Copper pairs cannot be at the same point.[8] As a result of this, the pair is broken up.

[8]Since the spin part of the wavefunction is symmetric, the space part must be antisymmetric, thus probability of finding the paired electrons vanishes at the same point.

3.3 Effects of Nonmagnetic Impurities on Anisotropic Superconductors

As has been pointed out in the previous section that the thermodynamic properties of isotropic BCS superconductors are not effected in the presence of nonmagnetic impurities. In this section, dependence of properties of *anisotropic* superconductors, mainly critical temperature and energy gap, on the impurity concentration[84,89,92-95,122,123] is studied. The derivation is limited to weak anisotropic pairing and only mean free path effects are taken into account.[9]. At the end of this section, effects of strong anisotropy (d, extented s and d+s pairing symmetries) are summarized.

First of all, the effect of weak anisotropy in the pure superconductor[91] is briefly discussed. This is important, because the properties of impure superconductors are expressed in terms of the characteristics of a pure superconductors. Let us introduce an effective electron-electron interaction of the following form

$$V(\mathbf{p},\mathbf{p}') = V_0[1 + \Omega(\mathbf{p},\mathbf{p}')], \tag{3.33}$$

where the quantity $\Omega(\mathbf{p},\mathbf{p}')$ describes the anisotropy of the interaction and it is chosen so that its average satisfies

$$< \Omega >= \int\int d\mathbf{p}d\mathbf{p}'\ \Omega(\mathbf{p},\mathbf{p}') = 0.$$

The interaction (3.33) is constant over the energy interval of width $2\omega_D$ at the Fermi surface, but depends on the angle between $\mathbf{p}$ and $\mathbf{p}'$ and the order parameter $\Delta(\mathbf{p})$ depends on orientation. Assuming that the anisotropy is small, namely

$$|\Omega(\mathbf{p},\mathbf{p}')| \ll 1. \tag{3.34}$$

Near the transition temperature, $\Delta(\mathbf{p})$ satisfies the linear integral equation

[9]See Ref. 92, for the more general case.

$$\Delta(\mathbf{p}) = T\sum_{\omega_n}\int \frac{d\mathbf{p}}{(2\pi)^3}\, V(\mathbf{p},\mathbf{p}')\, G_0(\mathbf{p},\omega_n)\, G_0(-\mathbf{p}',-\omega_n)\, \Delta(\mathbf{p}'). \tag{3.35}$$

Since the momentum integral contributes only very near the Fermi surface, it can be written as

$$\int \frac{d\mathbf{p}}{(2\pi)^3} = N(0)\int\int d\sigma d\xi(\mathbf{p}), \tag{3.36}$$

where $N(0) = mp_F/2\pi^2$ is the density of states at the Fermi level[10] and $d\sigma$, normalized to unity, is a dimensionless element of area on the Fermi surface.
In Eq. (3.35) G_0 is the Green's function for the electrons in the normal state and it is given by

$$G_0(\mathbf{p},\omega_n) = \frac{1}{i\omega_n - \xi(\mathbf{p})}, \tag{3.37}$$

where $\omega_n = (2n+1)\pi T$ and $\xi(\mathbf{p})$ is the energy measured from Fermi surface in the direction of the vector $\mathbf{p}$.
The frequency, ω_n, summation in (3.35) can be carried out easily (See for example Ref. 97) to give

$$\Delta(\tilde{\mathbf{p}}) = N(0)\int_0^{w_D} d\xi(\mathbf{p}')\frac{\tanh[\xi(\mathbf{p}')/2T]}{\xi(\mathbf{p}')}\int d\sigma' V(\tilde{\mathbf{p}},\tilde{\mathbf{p}}')\Delta(\tilde{\mathbf{p}}'). \tag{3.38}$$

Here $\tilde{\mathbf{p}}$ denotes a vector lying on the Fermi surface. Since the result of the integration is logarithmic, one can replace ω_D by some average frequency $\bar{\omega}_0$, then (3.38) becomes

$$\Delta(\tilde{\mathbf{p}}) = N(0)\ln\left(\frac{2\bar{w}_0\gamma}{\pi T}\right)\int d\sigma' V(\tilde{\mathbf{p}},\tilde{\mathbf{p}}')\Delta(\tilde{\mathbf{p}}'), \tag{3.39}$$

where $\ln\gamma = 0.577$. This linear homogeneous integral equation can be solved in the limit of weak anisotropy. Let us introduce the following expressions:

[10]We note that if a more realistic model for density of state is used, e. g. $N(0;\mathbf{p},\mathbf{p}') = N(0)[1+\xi(\mathbf{p},\mathbf{p}')]$, then the results are not changed significantly. See Ref. 92.

$$\begin{aligned}
&\Delta(\hat{\mathbf{p}}) = \Delta_0 + \Delta_1(\hat{\mathbf{p}}) \\
&\int d\sigma \Delta_1(\hat{\mathbf{p}}) = 0 \\
&\int d\sigma' \Omega(\hat{\mathbf{p}}, \hat{\mathbf{p}}') = \Omega_r(\hat{\mathbf{p}}) \\
&\int d\sigma \Omega(\hat{\mathbf{p}}, \hat{\mathbf{p}}') = \Omega_l(\hat{\mathbf{p}}') \\
&\int d\sigma \Omega_r(\hat{\mathbf{p}})\ \Omega_l(\hat{\mathbf{p}}) = \chi \\
&\lambda = \ V_0 N(0) \\
&\omega = \frac{2\bar{\omega}_0 \gamma}{\pi}.
\end{aligned} \tag{3.40}$$

Inserting (3.40) into (3.39)

$$\Delta_0 + \Delta_1(\hat{\mathbf{p}}) = \lambda \ln(\omega/T) \int d\sigma' [1 + \Omega(\hat{\mathbf{p}}, \hat{\mathbf{p}}')] [\Delta_0 + \Delta_1(\hat{\mathbf{p}})]. \tag{3.41}$$

Integrating both sides of (3.41) over $d\sigma$ and substituting the resulting expression into (3.41) it becomes

$$\Delta_1(\hat{\mathbf{p}}) = \lambda \ln(\omega/T)\ [\Delta_0 \Omega_r(\hat{\mathbf{p}}) + \int d\sigma' \{\Omega(\hat{\mathbf{p}}, \hat{\mathbf{p}}') - \Omega_l(\hat{\mathbf{p}}')\} \Delta_1(\hat{\mathbf{p}}')]. \tag{3.42}$$

By using the condition of weak anisotropy ($\Delta_1 \ll \Delta_0$) and hence neglecting the second term in the right hand side of (3.42)

$$1 = \lambda \ln(\omega/T)\ [1 + \lambda \ln(\omega/T)\ \chi]. \tag{3.43}$$

Eq. (3.43) determines the transition temperature, T_c, of pure superconductors to first order in the anisotropy χ, namely[11]

$$T_{c0} = \frac{2\bar{\omega}_0 \gamma}{\pi} \exp\left\{-\frac{(1-\chi)}{V_0 N(0)}\right\} = T_{c0}^{BCS} e^{\chi / V_0 N(0)}. \tag{3.44}$$

If the anisotropy is neglected so that $\chi = 0$ then (3.44) reduces to the BCS solution.

[11] A similar expression has been obtained by Markowitz and Kadanoff in Ref. 92.

It is important to note that as can be seen in (3.44), the anisotropy in the pairing interaction[12] always enhances the transition temperature by a factor of $e^{\chi/V_0 N(0)}$. Similar results are recently found in Ref. 98,99.

The anisotropy of order parameter can be calculated to the first order in χ, to give

$$\chi = \frac{\int d\sigma |\Delta(\tilde{\mathbf{p}})|^2}{|\Delta_0|^2} - 1 = \frac{\int d\sigma |\Delta_1(\tilde{\mathbf{p}})|^2}{|\Delta_0|^2} = \frac{<\Delta^2>}{<\Delta>^2} - 1 \tag{3.45}$$

Notice that, the result obtained in (3.45) justifies the original assumption of weak anisotropy in the gap, e. i. $\Delta_1 \ll \Delta_0$, if $\Omega(\mathbf{p},\mathbf{p}') \ll 1$.

Now it is the time to discuss the effects of nonmagnetic impurities on anisotropic superconductors. Abrikosov and Gor'kov[84,89] have shown that in the presence of impurities there again exists an equation of the form (3.35), which must be averaged over the positions of the impurities. This leads to the following equation

$$\Delta(\mathbf{p}) = T\sum_{\omega_n} \int \frac{d\mathbf{p}}{(2\pi)^3}\, \tilde{V}(\mathbf{p},\mathbf{p}')\, G_0^{\prime\tau}(\mathbf{p},w_n)\, G_0^{\prime\tau}(-\mathbf{p}',-\omega_n)\, \Delta(\mathbf{p}'), \tag{3.46}$$

where

$$\begin{aligned}
&G_0^{\prime\tau}(\mathbf{p},\omega_n) = \frac{1}{i\omega_n\eta - \xi(\mathbf{p})} \\
&\eta = 1 + \frac{n_i\pi N(0)}{|\omega_n|}\int d\sigma' |u(\check{\mathbf{p}},\tilde{\mathbf{p}}')|^2 = 1 + \frac{\Gamma}{2|\omega_n|} \\
&\tilde{V}(\mathbf{p},\mathbf{p}') = V(\mathbf{p},\mathbf{p}') \\
&\qquad + n_i \int \frac{d\mathbf{q}}{(2\pi)^3}\, \tilde{V}(\mathbf{p},\mathbf{q})\, G_0^{\prime\tau}(\mathbf{q},\omega_n)\, G_0^{\prime\tau}(-\mathbf{q},-\omega_n)\, |u(\mathbf{p},\mathbf{q})|^2.
\end{aligned} \tag{3.47}$$

Here n_i is the impurity concentration, u is the interaction potential of an electron with an impurity atom and $\Gamma = \pi n_i N(0) < u^2 >$. In the isotropic scattering case, the equation for $\tilde{V}$ is solved in the following form

$$\tilde{V}(\tilde{\mathbf{p}},\tilde{\mathbf{p}}') = V(\tilde{\mathbf{p}},\tilde{\mathbf{p}}') + \frac{\Gamma V_r(\tilde{\mathbf{p}})}{2|\omega_n|}, \tag{3.48}$$

[12]The origin of the pairing interaction can be phononic, magnetic or any others.

where

$$V_r(\hat{\mathrm{p}}) = \int d\sigma' V(\hat{\mathrm{p}}, \hat{\mathrm{p}}').$$

Adding and subtracting the term VG_0G_0 to the kernel of (3.46), the sum over ω_n and the integral over ξ can be calculated. First integrate the remaining difference over ξ, and express the summation over ω_n in terms of the logarithmic derivative of the Γ function. This gives us an integral equation similar to (3.39)

$$\begin{aligned}\Delta(\hat{\mathrm{p}}) &= \frac{\lambda}{V_0}\ln(w/T_c)\int d\sigma' V(\hat{\mathrm{p}},\hat{\mathrm{p}}')\Delta(\hat{\mathrm{p}}) \\ &\quad -\frac{\lambda}{V_0}K(2\pi T_c/\Gamma)\int d\sigma'\left[V(\hat{\mathrm{p}},\hat{\mathrm{p}}') - V_r(\hat{\mathrm{p}}')\right]\Delta_1(\hat{\mathrm{p}}'),\end{aligned} \tag{3.49}$$

where $K(\nu)$ can be written in terms of di-gamma function, namely

$$K(\nu) = 2\sum_{n>0}\frac{1}{(2n+1)[1+\nu(2n+1)]} = \Psi\left(\frac{1}{2}+\frac{1}{2\nu}\right) - \Psi\left(\frac{1}{2}\right). \tag{3.50}$$

Using the same procedure as pure case, for weak anisotropy, it is obtained that

$$1 = \lambda\ln(w/T)\,(1 + [\lambda\ln(w/T) - \lambda K(\nu)]\,\chi). \tag{3.51}$$

Combining (3.44) and (3.51), this leads to the final equation

$$\ln\left(\frac{T_{c0}}{T_c}\right) = \frac{\chi}{1+\chi}\left[\Psi\left(\frac{1}{2}+\frac{\alpha T_{c0}}{2\pi T_c}\right) - \Psi\left(\frac{1}{2}\right)\right] \tag{3.52}$$

where $\alpha = \Gamma/T_{c0}$ is the pair breaking parameter.

It can be easily seen from the foregoing equation that if anisotropy is zero ($\chi = 0$), then the critical temperature does not change ($T_c = T_{c0}$). Therefore, impurities have no effects on the superconductivity as pointed out in the previous section. Inserting (3.45) into (3.52), the following expression is obtained:

$$\ln\left(\frac{T_{c0}}{T_c}\right) = \left[1 - \frac{<\Delta>^2}{<\Delta^2>}\right]\left[\Psi\left(\frac{1}{2}+\frac{\alpha T_{c0}}{2\pi T_c}\right) - \Psi\left(\frac{1}{2}\right)\right]. \tag{3.53}$$

In Fig. 3.1, dependence of the transition temperature on the pair breaking parameter is plotted for different values of the anisotropy χ. The critical

temperature suppression increases the anisotropy of the order parameter. Many unusual properties of the high-T_c superconductors may be explained in terms of anisotropic order parameter (See Ref. 95 for further discussion).

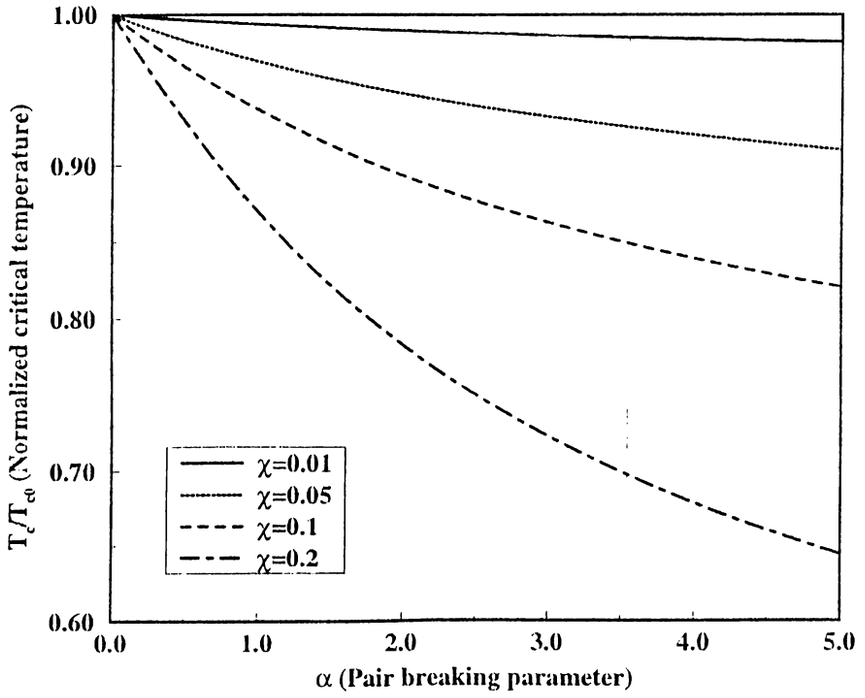

Figure 3.1: Dependence of the transition temperature on the pair breaking parameter for different values of the anisotropy χ.

For small and large concentrations of impurities, by using asymptotic forms of (3.50),

$$K(\nu) \sim \begin{pmatrix} \frac{\pi^2}{4\nu} & \text{for } \nu \gg 1 \\ \ln\left(\frac{2\gamma}{\nu}\right) & \text{for } \nu \ll 1 \end{pmatrix}. \tag{3.54}$$

the following expressions are obtained

$$\frac{T_c}{T_{c0}} \approx \begin{pmatrix} 1 - \frac{\pi}{8\tau T_{c0}}\chi & \text{for } \tau T_c \gg 1 \\ \left(\frac{\gamma}{\pi\tau T_{c0}}\right)^{-\chi} & \text{for } \tau T_c \ll 1 \end{pmatrix}. \tag{3.55}$$

Eq. (3.53) has been widely used to analyze the sensitivity of superconducting properties to the disorders[13] in high-T_c superconductors. In the literature, some authors[100-102] have used Eq. (3.52) incorrectly to study d-wave superconductors. This equation has been derived under the assumption of a weak anisotropy ($\chi \ll 1$). For the d-wave superconductors, since $< \Delta >= 0$, χ becomes infinite. This also causes infinite critical temperature as seen from Eq. (3.44) (For more extensive discussion, see Refs. 107,108). Therefore, Eq. (3.53) cannot be used for d-wave superconductors. However, it can be used for extended s-wave which has an anisotropy around $\chi \sim 0.2$.

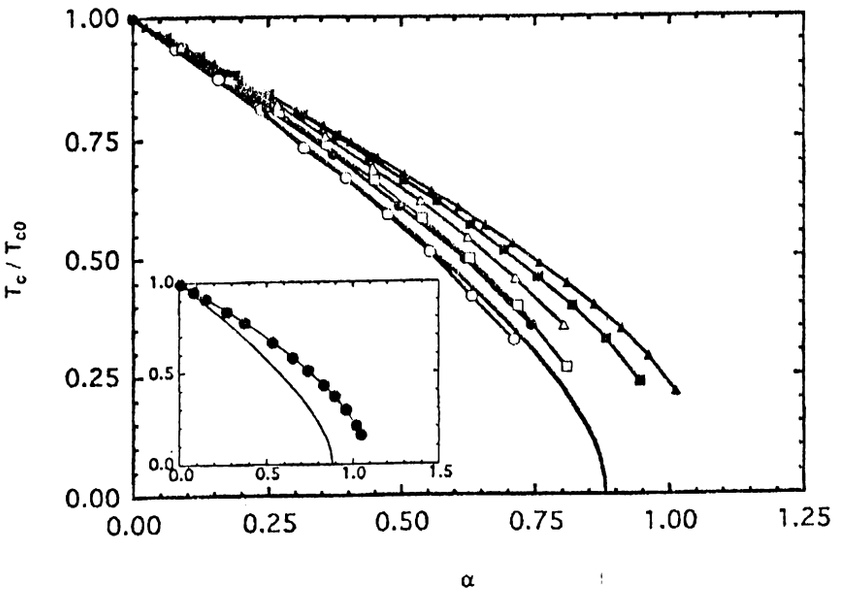

Figure 3.2: Normalized critical temperature T_c/T_{c0} versus the pair breaking parameter α for d-wave superconductors. In the figure, solid line, open symbols and solid symbols denote the AG equation, weak-coupling and strong-coupling t-matrix calculations respectively. [inset] Corresponding results predicted by the Monthoux-Pines model.

On the other hand, the results of t-matrix calculations[103-105] for d-wave

[13]Disorder can be induced by substitution or by irradiation.

approximately obey the Abrikosov-Gorkov (AG) equation[89]:

$$\ln\left(\frac{T_{c0}}{T_c}\right) = \Psi\left(\frac{1}{2}+\frac{\alpha T_{c0}}{2\pi T_c}\right) - \Psi\left(\frac{1}{2}\right) \tag{3.56}$$

From Eq. (3.56), it follows that T_c is completely suppressed at a critical pair breaking parameter $\alpha = 0.88$ $[T_c(\alpha_c) = 0]$. Figure 3.2 shows the comparison between t-matrix (for both weak- and strong-coupling limits) and AG results. In the inset to Fig. 3.2, the results are obtained in the Monthoux-Pines[106] model by solving the exact Eliashberg equations.

The similar forms of the foregoing equation have been obtained in Refs. 108-110 by using different methods. Beside this, very recently Golubov and Mazin[111] have proved that the superconductivity suppression by magnetic and nonmagnetic impurities is exactly the same when the average order parameter is zero (e. g. in case of d-wave pairing).

A brief discussion about breakdown of Eq. (3.56) for the short coherence length will be given in the Chapter 4.

As has been pointed out in Chapter 2, due to the orthorhombicity of some high-T_c materials (like YBCO), an admixture of s and d-waves is possible. Many authors[108,112,113] have studied impurity effects on the s+d-wave. They have very similar[14] results for T_c suppression:

$$(1+2\kappa^2)\ln\left(\frac{T_{c0}}{T_c}\right) = \Psi\left(\frac{1}{2}+\frac{\alpha T_{c0}}{2\pi T_c}\right) - \Psi\left(\frac{1}{2}\right) \tag{3.57}$$

In this case, the order parameter has the form $\Delta(\mathbf{p}) = \Delta_0[\cos 2\phi + \kappa]$. Note that it gives the d-wave T_c equation (3.56) when $\kappa = 0$. Figure 3.3 shows the T_c reduction curves for a s+d-wave superconductor as a function of the pair breaking parameter α for various values of the κ. Note that, as shown in Fig. 3.3, further impurity scattering does not affect T_c any more. This can be understood from the discussion in the previous section. While d-wave component of the order parameter is suppressed very rapidly, on the contrary, s-wave component is not

[14]In Refs. 108,113 the long T_c tail is found contrary to the Ref. 112 they have found that at some critical impurity concentration T_c completely vanishes.

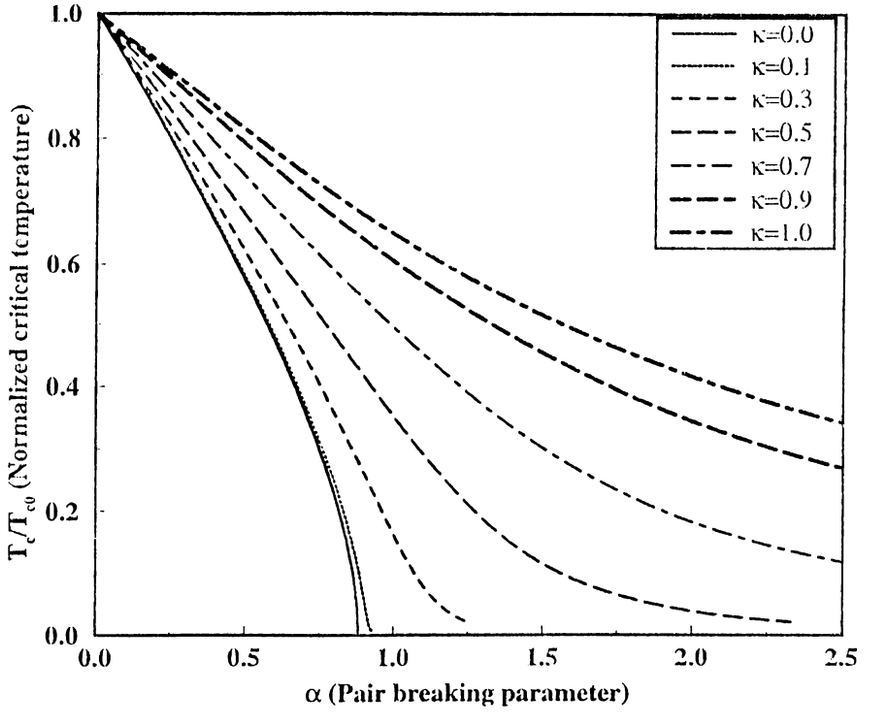

Figure 3.3: Normalized critical temperature T_c/T_{c0} as a function of the pair breaking parameter α for s+d-wave superconductor for the different values of κ.

affected from the impurities. The similar result will be obtained in Chapter 4 from the solution of BdG equations.

To sum up, the suppression of the critical temperature T_c in high-T_c cuprates is strongly related to anisotropy χ of the order parameter symmetry. For the s-wave $\chi = 0$, hence $\delta T_c = 0$. For the extended s-wave χ is small, therefore the critical temperature is suppressed very slowly. Since χ is large for d-wave, the critical temperature is suppressed very rapidly.

Chapter 4

INFLUENCE OF IMPURITY SUBSTITUTIONS ON THE HIGH-TEMPERATURE OXIDE SUPERCONDUCTORS

4.1 The Bogoliubov-de Gennes Equations for Two-dimensional Lattice

As has been pointed out in Chapter 2, high-T_c oxide superconductors have planar structure. Superconductivity occurs in the CuO_2 planes. Therefore, in this section we will drive the Bogoliubov-de Gennes equations for a two-dimensional lattice.

To model decoupled CuO_2 layers (See Fig. 4.1) in high-T_c cuprates, we consider a single-band Hamiltonian on a two-dimensional (2D) square lattice with

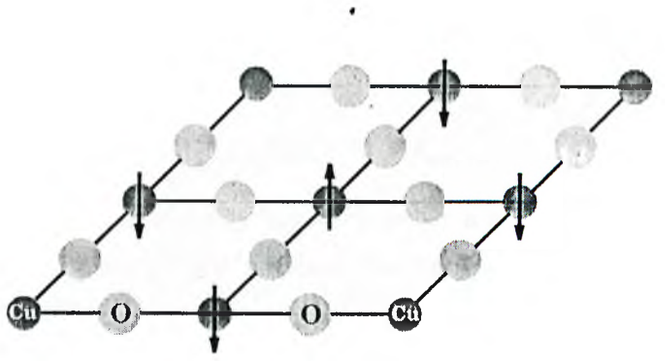

Figure 4.1: CuO_2 plane in the high-T_c oxide superconductors.

nearest-neighbor hopping along with onsite and nearest-neighbor interactions:

$$\begin{aligned} H &= -t \sum_{<ij>\sigma} c^{\dagger}_{i\sigma} c_{j\sigma} - \sum_{i\sigma} (\mu_i - V_i^{imp})\, n_{i\sigma} \\ &\quad + W_0 \sum_i n_{i\uparrow} n_{i\downarrow} + \frac{W_1}{2} \sum_{<ij>\sigma\sigma'} n_{i\sigma} n_{j\sigma'}. \end{aligned} \tag{4.1}$$

Here t denotes the hopping amplitude[1], i and j are site labels, $< ij >$ stands for nearest-neighbor pairs, σ is spin index ($\sigma = \uparrow$ or $\downarrow$), the operator $c^{\dagger}_{i\sigma}$ [$c_{i\sigma}$] creates [annihilates] a particle at site i with spin σ, $n_{i\sigma} = c^{\dagger}_{i\sigma} c_{i\sigma}$ is the electron number operator at site i, μ_i is the chemical potential of site i. V_i^{imp} is the impurity potential and it is nonzero for a set of randomly chosen sites (with density n_{imp}) and $V_i^{imp} = 0$ on all other sites. W_0 and W_1 are the onsite and nearest-neighbor interactions, respectively.[2] Similar Hamiltonians have been used by many authors to study the vortex structure,[78,72] impurities[65-68] and twin boundaries[81] in the d-wave superconductors. In Ref. 126, there is an extensive discussion on this type of local electron pairing models.

[1] In the presence of magnetic field, the hopping amplitude can be written as follows: $t_{ij} = t \exp\left[-ie/\hbar c \int_i^j d\mathbf{r} \cdot \mathbf{A}(\mathbf{r})\right]$, where $\nabla \times \mathbf{A} = \mathbf{B}$.

[2] In (4.1), we assume that ❶ V_i^{imp} is spin independent (nonmagnetic impurities, e. g. Zn) ❷ electron-electron coupling is independent of spin (as in the case nonmagnetic materials)

We use the following model for the impurity potential:

$$V_i^{imp} = V_0 \delta_{\mathbf{r},\mathbf{r}_i} + V_1 \delta_{\mathbf{r},\mathbf{r}_i+\delta}. \tag{4.2}$$

Here $\delta = \pm\mathbf{x}, \pm\mathbf{y}$ are nearest-neighbor vectors for a square lattice. Since high-T_c materials have highly correlated antiferromagnetic nature in normal state, the impurity atoms will produce distortions[155] in the magnetic correlations at the range of antiferromagnetic coherence length ($\xi_{AFM} = 3a$)[125] . As a result of this, finite-ranged potentials may be a reason for rapid suppression of the critical temperature in the oxide superconductorsçbalatsky93,xiang95.

The operators in (4.1) $c_{i\sigma}^\dagger$ and $c_{j\sigma'}$ satisfy the anticommutation rules

$$\begin{aligned} \left[c_{i\sigma}^\dagger, c_{j\sigma'}\right]_+ &= c_{i\sigma}^\dagger c_{j\sigma'} + c_{j\sigma'} c_{i\sigma}^\dagger = \delta_{i,j}\delta_{\sigma,\sigma'} \\ \left[c_{i\sigma}^\dagger, c_{j\sigma'}^\dagger\right]_+ &= 0 \\ \left[c_{i\sigma}, c_{j\sigma'}\right]_+ &= 0. \end{aligned} \tag{4.3}$$

The interaction terms in (4.1) can be replaced by average potentials acting on one particle at a time, and hence they reduce to two operator terms. The effective Hamiltonian takes the following form

$$\begin{aligned} H_{eff} &= -t \sum_{<ij>\sigma} c_{i\sigma}^\dagger c_{j\sigma} - \sum_{i\sigma} (\mu_i - V_i^{imp}) c_{i\sigma}^\dagger c_{i\sigma} + \sum_{i\sigma} U_0^i \; c_{i\sigma}^\dagger c_{i\sigma} \\ &+ \sum_{<ij>\sigma} U_1^j \; c_{i\sigma}^\dagger c_{i\sigma} + \sum_{<ij>\sigma} U_1^{ij} \; c_{i\sigma}^\dagger c_{j\sigma} \\ &+ \sum_i (\Delta_0^i \; c_{i\uparrow}^\dagger c_{i\downarrow}^\dagger + \Delta_0^{i*} \; c_{i\downarrow} c_{i\uparrow}) + \sum_{<ij>} (\Delta_s^{ij} \; c_{i\uparrow}^\dagger c_{j\downarrow}^\dagger + \Delta_s^{ij*} \; c_{j\downarrow} c_{i\uparrow}). \end{aligned} \tag{4.4}$$

Assuming that H_{eff} is known, we determine its eigenstates and corresponding energies. Since H_{eff} is a quadratic form in c and $c^\dagger$, we can diagonalize it by using Bogoliubov transformations

$$c_{i\downarrow} = \sum_n \gamma_{n\uparrow} \; u_n^i - \gamma_{n\downarrow}^\dagger \; v_n^{i*}$$

$$c_{i\downarrow} = \sum_n \gamma_{n\downarrow}\, u_n^i + \gamma_{n\downarrow}^\dagger\, v_n^{i*}, \tag{4.5}$$

where the γ and $\gamma^\dagger$ are new operators still satisfying the fermionic commutation relations

$$\begin{aligned}
\left[\gamma_{m\sigma}^\dagger, \gamma_{n\sigma'}\right]_+ &= \gamma_{m\sigma}^\dagger \gamma_{n\sigma'} + \gamma_{n\sigma'}\gamma_{m\sigma}^\dagger = \delta_{mn}\delta_{\sigma\sigma'} \\
\left[\gamma_{m\sigma}^\dagger, \gamma_{n\sigma'}^\dagger\right]_+ &= 0 \\
\left[\gamma_{m\sigma}, \gamma_{n\sigma'}\right]_+ &= 0.
\end{aligned} \tag{4.6}$$

This transformations lead to an the effective Hamiltonian H_{eff} that becomes diagonal:

$$H_{eff} = \epsilon_0 + \sum_{n\sigma} \epsilon_n \gamma_{n\sigma}^\dagger \gamma_{n\sigma}, \tag{4.7}$$

where ϵ_0 and ϵ_n are the ground and n^{th} excited states energies of the H_{eff} respectively. Taking the commutator of H_{eff} with $\gamma_{n\sigma}^\dagger$ and $\gamma_{n\sigma}$, we get

$$[\gamma_{n\sigma}, H_{eff}] = \epsilon_n \gamma_{n\sigma}$$

$$[\gamma_{n\sigma}^\dagger, H_{eff}] = -\epsilon_n \gamma_{n\sigma}^\dagger. \tag{4.8}$$

Equation (4.8) fixes the functions u_n and v_n in (4.5). To find the equations for u_n and v_n, we calculate the commutator $[c, H_{eff}]$. By using the definition (4.4) of H_{eff} and the anticommutation

relations(4.3) of c operators, we obtain

$$\begin{aligned}
[c_{i\downarrow}, H_{eff}] &= -\sum_\delta \left(t - U_1^{i,i+\delta}\right) c_{i+\delta\downarrow} - \left(\mu_i - V_i^{imp} - U_0^i - \sum_\delta U_1^{i+\delta}\right) c_{i\downarrow} \\
&\quad + \Delta_0^i\, c_{i\downarrow}^\dagger + \sum_\delta \Delta_\delta^{i,i+\delta}\, c_{i+\delta\downarrow}^\dagger \\
\left[c_{i\downarrow}^\dagger, H_{eff}\right] &= \sum_\delta \left(t - U_1^{i,i+\delta}\right) c_{i+\delta\downarrow}^\dagger + \left(\mu_i - V_i^{imp} - U_0^i - \sum_\delta U_1^{i+\delta}\right) c_{i\downarrow}^\dagger \\
&\quad + \Delta_0^{i*}\, c_{i\downarrow} + \sum_\delta \Delta_\delta^{i,i+\delta*}\, c_{i+\delta\downarrow}.
\end{aligned} \tag{4.9}$$

In (4.9), we replace the c's by the γ's by using (4.5). Then we apply the commutation relations (4.8). Comparing the coefficients of γ_n on both sides of the equations, we obtain the Bogoliubov-de Gennes(BdG

) equations:

$$\begin{aligned}
\epsilon_n u_n^i &= -\sum_\delta \left(t - U_1^{i,i+\delta}\right) u_n^{i+\delta} - \left(\mu_i - V_i^{imp} - U_0^i - \sum_\delta U_1^{i+\delta}\right) u_n^i \\
&\quad +\Delta_0^i\, v_n^i + \sum_\delta \Delta_\delta^{i,i+\delta}\, v_n^{i+\delta} \\
\epsilon_n v_n^i &= \sum_\delta \left(t - U_1^{i,i+\delta}\right) v_n^{i+\delta} + \left(\mu_i - V_i^{imp} - U_0^i - \sum_\delta U_1^{i+\delta}\right) v_n^i \\
&\quad +\Delta_0^{i*} u_n^i + \sum_\delta \Delta_\delta^{i,i+\delta *} u_n^{i+\delta}. \qquad (4.10)
\end{aligned}$$

Now, the effective potentials U_0^i, U_1^i, $U_1^{i,i+\delta}$, Δ_0^i and $\Delta_\delta^{i,i+\delta}$ can be determined by minimizing the Gibbs free energy of the system:

$$\mathcal{F} = < H > - TS, \qquad (4.11)$$

where T is the temperature, S is the entropy of the system and $< H >$ is the mean value of (4.1), given by

$$\begin{aligned}
< H > &= -t \sum_{<ij>\sigma} < c_{i\sigma}^\dagger c_{j\sigma} > - \sum_{i\sigma} (\mu_i - V_i^{imp}) \; < c_{i\sigma}^\dagger c_{i\sigma} > \\
&\quad + W_0 \sum_i \; < c_{i\uparrow}^\dagger c_{i\downarrow}^\dagger c_{i\downarrow} c_{i\uparrow} > + \frac{W_1}{2} \sum_{<ij>\sigma\sigma'} < c_{i\sigma}^\dagger c_{j\sigma'}^\dagger c_{j\sigma'} c_{i\sigma} > \qquad (4.12)
\end{aligned}$$

The product $< c^\dagger c^\dagger c\, c >$ can be simplified by using the Wick's theorem

$$\begin{aligned}
< c^\dagger(1) c^\dagger(2) c(3) c(4) > &= \quad < c^\dagger(1) c(4) >< c^\dagger(2) c(3) > \\
&\quad - < c^\dagger(1) c(3) >< c^\dagger(2) c(4) > \\
&\quad + < c^\dagger(1) c^\dagger(2) >< c(3) c(4) > . \qquad (4.13)
\end{aligned}$$

Eq.(4.11) becomes

$$\begin{aligned}\mathcal{F} &= -t\sum_{<ij>\sigma} < c^{\dagger}_{i\sigma}c_{j\sigma} > -\sum_{i\sigma}(\mu_i - V_i^{imp}) < c^{\dagger}_{i\sigma}c_{i\sigma} > \\ &+W_0\sum_i < c^{\dagger}_{i\uparrow}c_{i\uparrow} >< c^{\dagger}_{i\downarrow}c_{i\downarrow} > + < c^{\dagger}_{i\uparrow}c^{\dagger}_{i\downarrow} >< c_{i\downarrow}c_{i\uparrow} > \\ &+\frac{W_1}{2}\sum_{<ij>\sigma\sigma'}\Big[< c^{\dagger}_{i\sigma}c_{i\sigma} >< c^{\dagger}_{j\sigma'}c_{j\sigma'} > - < c^{\dagger}_{i\sigma}c_{j\sigma'} >< c^{\dagger}_{j\sigma'}c_{i\sigma} > \\ &\qquad + < c^{\dagger}_{i\sigma}c^{\dagger}_{j\sigma'} >< c_{j\sigma'}c_{i\sigma} >\Big] - TS. \qquad (4.14)\end{aligned}$$

Variation in $\mathcal{F}$ is

$$\begin{aligned}\delta\mathcal{F} &= -t\sum_{<ij>\sigma}\delta < c^{\dagger}_{i\sigma}c_{j\sigma} > -\sum_{i\sigma}(\mu_i - V_i^{imp})\,\delta < c^{\dagger}_{i\sigma}c_{i\sigma} > \\ &+W_0\sum_i \delta < c^{\dagger}_{i\uparrow}c_{i\uparrow} >< c^{\dagger}_{i\downarrow}c_{i\downarrow} > + < c^{\dagger}_{i\uparrow}c_{i\uparrow} > \delta < c^{\dagger}_{i\downarrow}c_{i\downarrow} > \\ &+W_0\sum_i \delta < c^{\dagger}_{i\downarrow}c^{\dagger}_{i\downarrow} >< c_{i\uparrow}c_{i\uparrow} > + < c^{\dagger}_{i\downarrow}c^{\dagger}_{i\downarrow} > \delta < c_{i\uparrow}c_{i\uparrow} > \\ &+\frac{W_1}{2}\sum_{<ij>\sigma\sigma'}\delta < c^{\dagger}_{i\sigma}c_{i\sigma} >< c^{\dagger}_{j\sigma'}c_{j\sigma'} > + < c^{\dagger}_{i\sigma}c_{i\sigma} > \delta < c^{\dagger}_{j\sigma'}c_{j\sigma'} > \\ &-\frac{W_1}{2}\sum_{<ij>\sigma\sigma'}\delta < c^{\dagger}_{i\sigma}c_{j\sigma'} >< c^{\dagger}_{j\sigma'}c_{i\sigma} > + < c^{\dagger}_{i\sigma}c_{j\sigma'} > \delta < c^{\dagger}_{j\sigma'}c_{i\sigma} > \\ &+\frac{W_1}{2}\sum_{<ij>\sigma\sigma'}\delta < c^{\dagger}_{i\sigma}c^{\dagger}_{j\sigma'} >< c_{j\sigma'}c_{i\sigma} > + < c^{\dagger}_{i\sigma}c^{\dagger}_{j\sigma'} > \delta < c_{j\sigma'}c_{i\sigma} > \\ &-T\delta S. \qquad (4.15)\end{aligned}$$

We note that the quantity

$$\tilde{\mathcal{F}} =< H_{eff} > -TS \qquad (4.16)$$

is stationary γ and $\gamma^{\dagger}$ diagonalize H_{eff} exactly. By using (4.4), this condition gives us

$$\begin{aligned}\delta\tilde{\mathcal{F}} &= 0 = \delta < H_{eff} > -T\delta S \\ &-t\sum_{<ij>\sigma}\delta < c^{\dagger}_{i\sigma}c_{j\sigma} > -\sum_{i\sigma}(\mu_i - V_i^{imp})\delta < c^{\dagger}_{i\sigma}c_{i\sigma} > + \sum_{i\sigma} U_0^i\,\delta < c^{\dagger}_{i\sigma}c_{i\sigma} >\end{aligned}$$

$$+\sum_{<ij>\sigma} U_1^{ij}\ \delta < c_{i\sigma}^\dagger c_{i\sigma} > + \sum_{<ij>\sigma} U_1^{ij}\ \delta < c_{i\sigma}^\dagger c_{j\sigma} >$$
$$+\sum_i (\Delta_0^i\ \delta < c_{i\downarrow}^\dagger c_{i\downarrow}^\dagger > + \Delta_0^{i*}\ \delta < c_{i\downarrow} c_{i\downarrow} >)$$
$$+\sum_{<ij>} (\Delta_\delta^i\ \delta < c_{i\downarrow}^\dagger c_{j\downarrow}^\dagger > + \Delta_\delta^{i*}\ \delta < c_{j\downarrow} c_{i+\delta\downarrow}) > -T\delta S. \tag{4.17}$$

Comparing (4.15) and (4.17), we see that F will be stationary if we take the effective potentials as

$$\begin{aligned}
U_0^i &= W_0 < c_{i\downarrow}^\dagger c_{i\downarrow} >= W_0 \sum_n \left(|u_n^i|^2 f_n + |v_n^i|^2 (1 - f_n) \right) \\
U_1^i &= W_1 < c_{i\downarrow}^\dagger c_{i\downarrow} >= W_1 \sum_n \left(|u_n^i|^2 f_n + |v_n^i|^2 (1 - f_n) \right) \\
U_1^{i,i+\delta} &= -W_1 < c_{i+\delta\downarrow}^\dagger c_{i\downarrow} >= -W_1 \sum_n \left(u_n^i u_n^{i+\delta *} f_n + v_n^i v_n^{i+\delta *} (1 - f_n) \right) \\
\Delta_0^i &= W_0 < c_{i\downarrow} c_{i\downarrow} >= -W_0 \sum_n u_n^i v_n^{i*} (1 - 2f_n) \\
\Delta_\delta^{i,i+\delta} &= \frac{W_1}{2} (< c_{i+\delta\downarrow} c_{i\downarrow} > - < c_{i\downarrow} c_{i+\delta\downarrow} >) \\
&= -\frac{W_1}{2} \sum_n \left(u_n^{i+\delta} v_n^{i*} + u_n^i v_n^{i+\delta *} \right) (1 - 2f_n).
\end{aligned} \tag{4.18}$$

The entropy S and the free energy $\mathcal{F}$ of the system can be written explicitly, by using mean values of γ's

$$\begin{aligned}
< \gamma_{m\sigma}^\dagger \gamma_{n\sigma'} > &= \delta_{mn} \delta_{\sigma\sigma'} f_n \\
< \gamma_{m\sigma} \gamma_{n\sigma'} > &= 0 \\
< \gamma_{m\sigma}^\dagger \gamma_{n\sigma'}^\dagger > &= 0,
\end{aligned} \tag{4.19}$$

where $f_n = \frac{1}{\exp(\epsilon_n / k_B T) + 1}$ turns out to be Fermi distribution function.

$$S = -k_B \sum_{n\sigma} f_n \ln f_n - (1 - f_n) \ln (1 - f_n). \tag{4.20}$$

From (4.11) and (4.19), we obtain

$$
\begin{aligned}
\mathcal{F} \;=\; & -4t\sum_{in\delta}\left(u_n^i u_n^{i+\delta^*} f_n + v_n^i v_n^{i+\delta^*}(1-f_n)\right) \\
& -2\sum_{in}(\mu_i - V_i^{imp})\left(|u_n^i|^2 f_n + |v_n^i|^2(1-f_n)\right) \\
& +W_0\sum_{imn}\left(|u_m^i|^2 f_m + |v_m^i|^2(1-f_m)\right)\left(|u_n^i|^2 f_n + |v_n^i|^2(1-f_n)\right) \\
& -W_0\sum_{imn}(u_m^i v_m^{i\,*}(1-2f_m))(u_n^{i\,*} v_n^i(1-2f_n)) \\
& +W_1\sum_{imn\delta}\left(|u_m^i|^2 f_m + |v_m^i|^2(1-f_m)\right)\left(|u_n^{i+\delta}|^2 f_n + |v_n^{i+\delta}|^2(1-f_n)\right) \\
& +2W_1\sum_{imn\delta}\left(u_m^{i\,*} v_m^{i+\delta} f_m - v_m^i u_m^{i+\delta^*}(1-f_m)\right)\left(u_n^i v_n^{i+\delta^*} f_n + u_n^{i+\delta} v_m^{i\,*}(1-f_n)\right) \\
& -2W_1\sum_{imn\delta}\left(u_m^{i\,*} u_m^{i+\delta} f_m + v_m^i v_m^{i+\delta^*}(1-f_m)\right)\left(u_n^i u_n^{i+\delta^*} f_n + v_n^{i+\delta} v_m^{i\,*}(1-f_n)\right) \\
& -k_B T\sum_{n\sigma} f_n \ln f_n - (1-f_n)\ln(1-f_n). \qquad (4.21)
\end{aligned}
$$

4.2 On the Numerical Solution of BdG Equations

To investigate the properties of high-T_c cuprate superconductors in the presence of impurities, we solve BdG equations (4.10) numerically with self-consistency conditions (4.18)[3] for different pairing symmetries. We take a square lattice with periodic boundary conditions. In the absence of impurities, BdG equations can be solved by considering translational invariance. In this case, we obtain the usual BCS excitation spectrum:

$$E(\mathbf{k}) = \sqrt{\xi(\mathbf{k})^2 + |\Delta(\mathbf{k})|^2}, \qquad (4.22)$$

where $\xi(\mathbf{k}) = -2t(\cos k_x + \cos k_y) - \mu$ and $\Delta(\mathbf{k})$ has different forms corresponding to various symmetries. For s-, extended s- and d-wave (See Fig. 4.2):

[3]Since the first two terms in (4.13) are nearly temperature independent, we take into account the last term only.

$$\Delta(\mathbf{k}) = \begin{cases} \Delta_0 & \text{for s-wave} \\ -2\Delta_s(\cos k_x + \cos k_y) & \text{for extended s-wave} \\ -2\Delta_d(\cos k_x - \cos k_y) & \text{for d-wave} \end{cases}, \qquad (4.23)$$

where Δ_0, Δ_s and Δ_d are computed numerically for given parameters W_0, W_1 and μ.

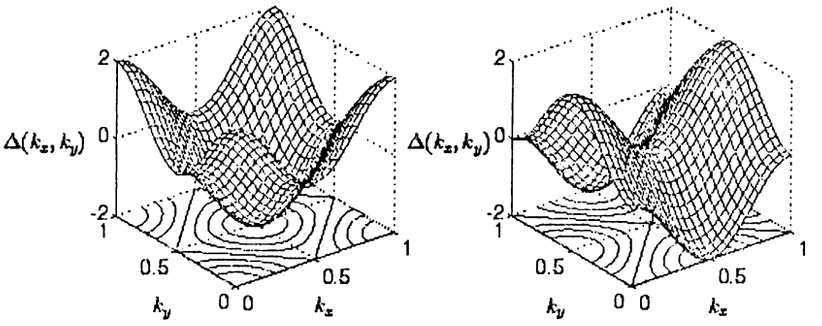

Figure 4.2: Plots of order parameters for extended s- and d-wave.

For a system of size L, we diagonalize $2L^2 \times 2L^2$ matrix for suitably chosen an initial guess for order parameter in different pairing symmetries. Then, we compute new values of the order parameters from Eq. 4.18 and we iterate this process until the desired convergence is achieved. Figure 4.3 shows the flow chart describing the computational procedure.

At this point, we give some remarks about general features of the solution:

- The physical properties, such as critical temperature T_c, order parameter Δ and coherence length ξ_0, are functions of the half-bandwidth ($= 4t$) and the electron concentration, instead of Debye frequency ω_D as in the BCS theory.

- The number of electrons per lattice site n is calculated from

$$n = \frac{1}{N}\sum_i < n_{i\uparrow} + n_{i\downarrow} >$$

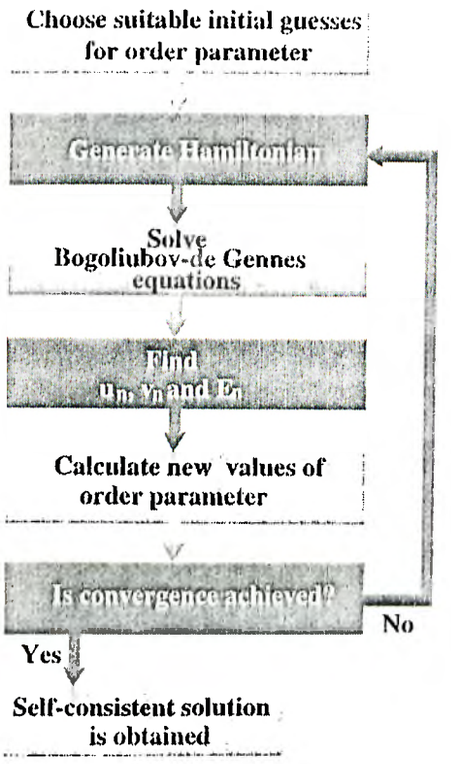

Figure 4.3: The flow chart describing the computational procedure.

$$= \frac{2}{N}\sum_{i,n}\left(|u_n^i|^2 f_n + |v_n^i|^2(1-f_n)\right) \qquad n \in [0,2], \quad (4.24)$$

where N is number of sites and $n_{i\sigma} = c_{i\sigma}^{\dagger}c_{i\sigma}$ is the number operator. As shown in Fig. 4.4, the order parameter is symmetric about half filling ($n = 1$) which reflect the electron-hole symmetry.

- In the presence of onsite repulsion ($W_0 > 0$) and nearest-neighbor attraction ($W_1 < 0$), the system favors the d-wave pairing for wide-range of parameters.

- Dependence of the order parameter on strength of the scattering potentials is shown in Fig. 4.5. Note that further increase of the strength of the potentials does not change the order parameter. For consistency with

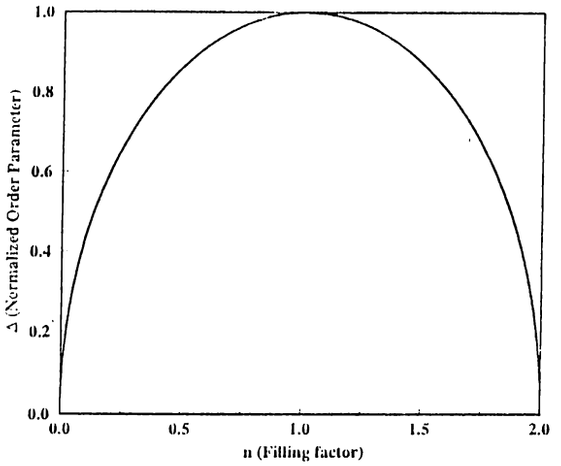

Figure 4.4: Dependence of the order parameter on number of electrons per lattice site.

the previous works, we call the scattering potential *unitary* ($V_0 \gg t$) or *subunitary* ($V_0 \sim t$).

- In the presence of impurities, the order parameter is averaged over many different impurity configurations. Most of our results are obtained by averaging over 10 different distributions. It should be noted that larger concentration of impurities leads to increase the number of iterations to achieved reasonable convergence (~ 50).

- The coherence length ξ_0 is a characteristic length scale for superconductors. If ξ_0 is comparable with dimension of the system, finite-size effects become important, then the required convergence can not be achieved. For this reason, we always take smaller coherence lengths much smaller compared to the size of the system.

- For the orthorhombic materials, we take $t_x = 1t$ and $t_y = 1.55t$ which ii estimated by using the observed a-b anisotropy in the magnetic penetration

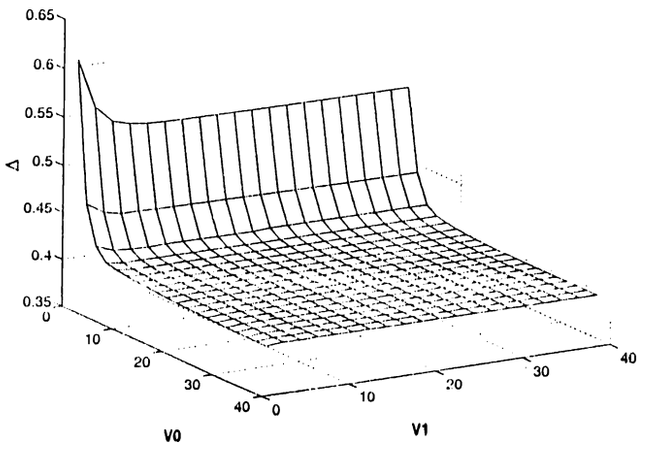

Figure 4.5: Dependence of the order parameter on the strength of the impurity potentials.

depths ($\lambda_a = 1600$ Åand $\lambda_b = 1030$ Å).[136]

➤ We take $t = 1$ in the calculations throughout this work.

4.3 Variation of Order Parameter in the Vicinity of a Single Impurity

In this section we study effects of an impurity on the order parameter in the CuO_2 plane. Byers and his co-workers[121] have investigated influence of an impurity on the nearby tunneling conductance in the anisotropic superconductors. They have shown that momentum-dependence of the superconducting gap $\Delta(k)$ can be determined from the spatial variation of the tunneling conductance. Franz and his co-workers[67] have also studied variations of order parameters in the presence of a single impurity in the d-wave superconductors.

Figures 4.6, 4.7, 4.9 and 4.8 show variation of the OPs in the vicinity of a

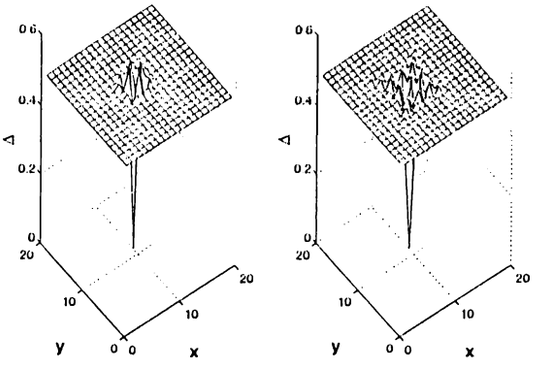

Figure 4.6: Variation of s-wave order parameter in the vicinity of an impurity located at the center of the lattice. $V_0 = 50t$, $V_1 = 0t$ for left panel and $V_0 = 50t$, $V_1 = 2t$ for right panel.

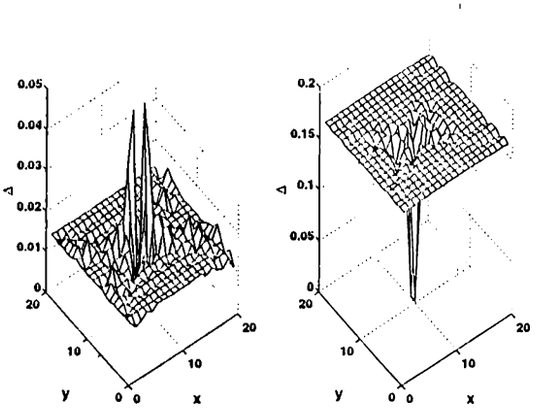

Figure 4.7: Variation of s+d-wave order parameter in the vicinity of an impurity located at the center of the lattice. s-wave component of the OP [left panel] and d-wave component of the OP [right panel] for $V_0 = 50t$, $V_1 = 2t$.

single impurity for s-, s+d-, d- ($\xi_0 = 2.6a$) and d-wave ($\xi_0 = 4a$), respectively. We should note that, as shown in these figures,

① the OP vanishes at the impurity site and recovers its bulk values over a distance ξ_0,

② for s+d-wave, s-wave component of the OP increases near the impurity site at which d-wave component vanishes (See Fig. 4.7).
③ the finite-ranged potentials affect the OPs much more near the impurity site (See Fig. 4.9 [left panel]),
④ as the coherence length increases, the effective range of a single impurity increases (Compare Figs. 4.9 and 4.8 [left panels]),
⑤ Δ is inversely proportional to the coherence length (Compare Figs. 4.9 and 4.8 [left panels]).

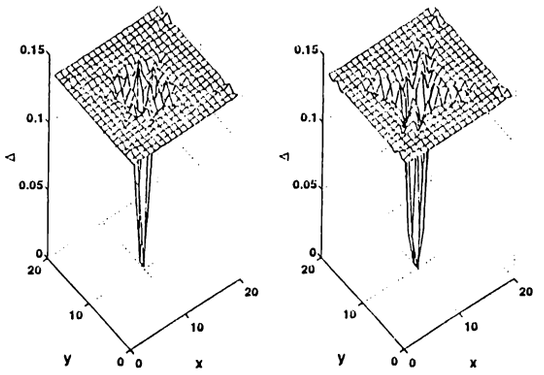

Figure 4.8: Variation of d-wave order parameter in the vicinity of an impurity located at the center of the lattice. $V_0 = 50t$, $V_1 = 0t$ for left panel and $V_0 = 50t$, $V_1 = 2t$ for right panel.

4.4 Determination of Coherence Length ξ and Critical Temperature T_c

In our calculations, the zero temperature coherence length is estimated from

$$\xi_0^2 \sim \sum_i r_i^2 \psi(i), \tag{4.25}$$

where r_i is the distance from the origin to site i, and $\psi(i)$ is given by

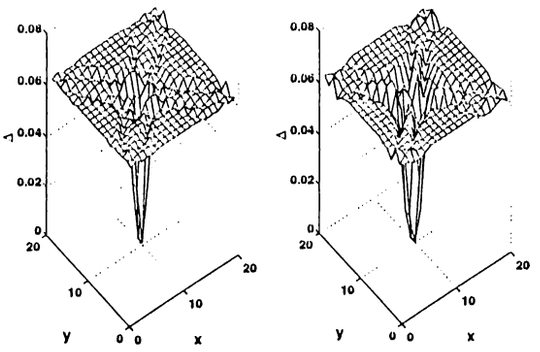

Figure 4.9: Variation of d-wave order parameter in the vicinity of an impurity located at the center of the lattice. $V_0 = 50t$, $V_1 = 0t$ for left panel and $V_0 = 50t$, $V_1 = 2t$ for right panel.

$$\psi(i) = \frac{|g(0,i)|^2}{\sum_i |g(0,i)|^2}, \tag{4.26}$$

here

$$|g(0,i)| = < c_{0\downarrow} c_{i\uparrow} > = \sum_n \left[u_n^i v_n^0 (1 - f_n) - u_n^0 v_n^i f_n \right]. \tag{4.27}$$

Amplitude of $g(0,i)$ is plotted in Fig. 4.10 and 4.11 for d- and s+d-wave, respectively. As shown in the Fig. 4.11, due to orthorhombicity ($a \neq b$), ξ_a and ξ_b have different values.

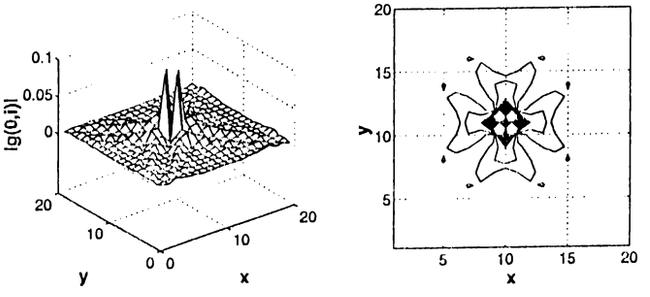

Figure 4.10: Amplitude of $g(0,i)$ for d-wave.

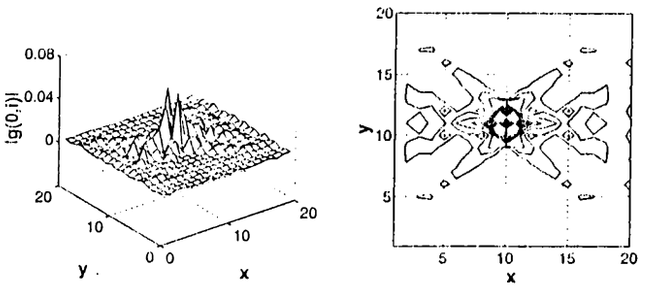

Figure 4.11: Amplitude of $g(0,i)$ for s+d wave.

The result is checked by examining the variation of the order parameter (at zero temperature) in the vicinity of a single impurity located at the center of the lattice (See Figs. 4.9 [left panel] and 4.12).

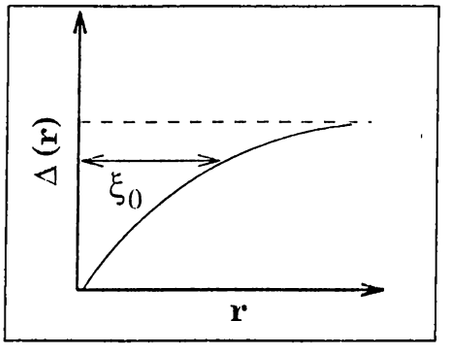

Figure 4.12: Order parameter vanish at the impurity site and recover its bulk values at a distance ξ_0.

In the BCS theory, the coherence length is given by

$$\xi_0 = \frac{\hbar v_F}{\pi \Delta} \sim \frac{W_{CB}}{\pi^2 \Delta} a \tag{4.28}$$

where W_{CB} is the bandwidth of the conduction band and a is the lattice constant. For large values of ξ_0, results of (4.25) and (4.28) are identical.

In Fig.4.13, we plot Δ versus the inverse coherence length $1/\xi_0$. For large values of the coherence length ($\xi_0 > 5a$), slope of the figure approaches to the

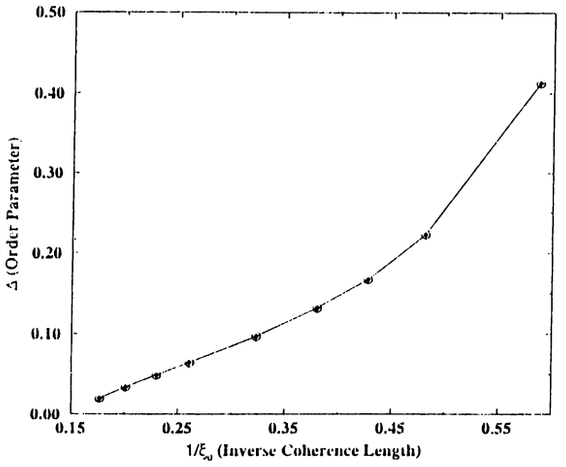

Figure 4.13: Order parameter versus inverse coherence length $1/\xi_0$.

BCS value, W_{CB}/π^2. On the other hand, when ξ_0 becomes smaller, the slope deviates significantly from the BCS prediction.

Determination of the critical temperature T_c is more complicated (especially in the presence of disorders). The Figures. 4.14 and 4.15 show temperature dependence of the OP in the absence of impurities and for various impurity concentrations, respectively. We know that the temperature dependence of coherence length is given by

$$\xi(T) \sim \xi(0)\left(1 - \frac{T}{T_c}\right)^{-1/2} \tag{4.29}$$

Near the transition temperature, the coherence length diverges and becomes larger than the system size. Hence, the correct solutions cannot be obtained. Considering this argument, we think that the results (Fig. 2) of Ref. 68 and their conclusion "the average zero-temperature gap does not scale with T_c, as one would expect from BCS theory" may be artifact. It is important to note that, the OP determines the basic specific features of superconductors: zero resistance and the Meissner effect. As long as OP is finite, these properties are observed.

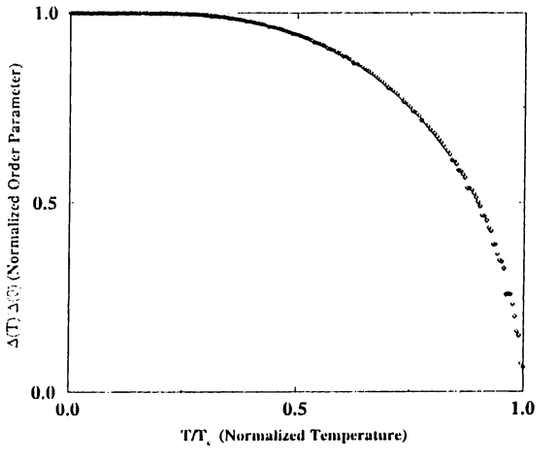

Figure 4.14: Temperature dependence of the d-wave OP in the absence of disorder.

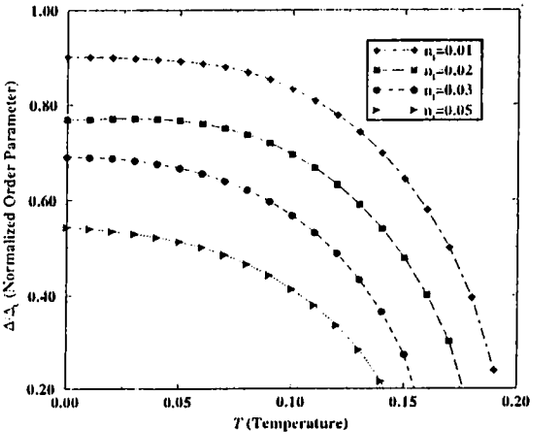

Figure 4.15: Temperature dependence of the d-wave OP for various values of impurity concentration.

At the same time, the energy gap may vanishes. This situation leads to gapless superconductivity. In fact, in the disordered systems energy gap does not coincide with the order parameter.[35,96]

4.5 Nonmagnetic Impurity Substitution in High-T_c Cuprates: Experimental Results

Numerous experimental investigations into the effects of the substitution of copper in the high-T_c oxide superconductors by 3d metallic elements (e. g. Zn, Ni, ...) have appeared in the literature. In the most of the experiments, effects of the Zn and Ni substitutions in Y-Ba-Cu-O,[141-143,61,144,146-150,139,52] La-Sr-Cu-O[152-154] and Bi-Sr-La-Cu-O[155] compounds have been investigated. The results of the experiment can be summarized as follows:

① The Zn substitution for Cu depresses the T_c of the high-temperature oxide superconductors much stronger than the Ni substitution (See Table 4.1).

② The Zn substitution results in a more drastic structure distortion than the Ni substitution.[155]

③ The growth in the normal state resistivity $d\rho_n/dx$ just above the critical temperature is quite similar for the Zn and Ni.

④ The Ni substitution leads to a orthorhombic-to-tetragonal structure transition.

⑤ At the larger concentration, the Zn ions start to occupy Cu-site in the chain.

Figures 4.16 and 4.17 show the transition temperature suppression due to Zn substitution in the Y-Ba-Cu-O and La-Sr-Cu-O compounds, respectively.

Table 4.1 displays the critical impurity concentration in the various substitution experiments.

4.6 Nonmagnetic Impurity Substitution in High-T_c Cuprates: Theoretical Calculations

Theoretical studies[139] underestimates the critical impurity concentration, at which the superconductivity vanishes completely [$T_c(n_c) = 0$], approximately by a factor of two or more in comparison with experimental results. More realistic

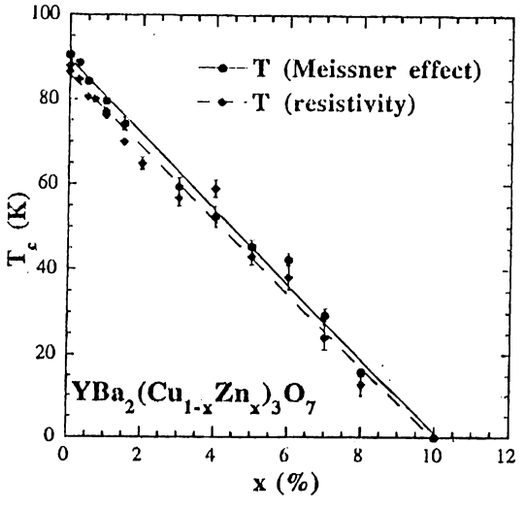

Figure 4.16: Dependence of the critical temperature on the Zn concentration in the Y-Ba-Cu-O compounds. Taken from Ref. 149.

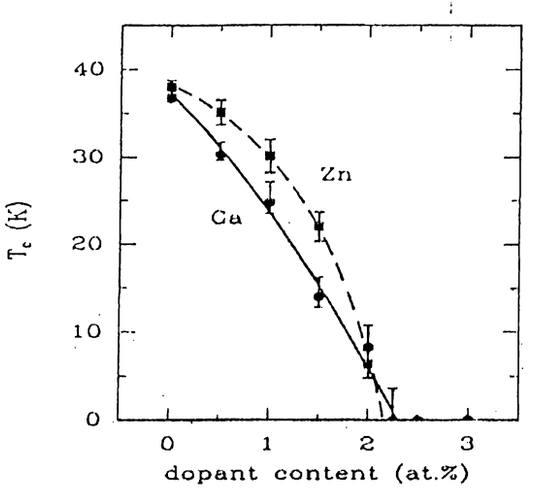

Figure 4.17: Dependence of the critical temperature on the Zn concentration in the La-Sr-Cu-O compounds. Taken from Ref. 152.

models have improved this contradiction slightly. We can summarize these model as follows:

Material	dT_c/dx	T_c [K]	n_c	Ref.
$YBa_2(Cu_{1-x}Zn_x)_3O_{6+y}$		94	0.1	141
$YBa_2(Cu_{1-x}Zn_x)_3O_7$	-13 K	92	0.12-0.13	43
$YBa_2(Cu_{1-x}Zn_x)_3O_{7-y}$		89	0.05-0.06	142
$YBa_2(Cu_{1-x}Zn_x)_3O_{7-\delta}$		92	0.07-0.08	143
$YBa_2Cu_{3-x}Zn_xO_{7-\delta}$	-3.7 K	90		61
$YBa_2(Cu_{1-x}Zn_x)_3O_{7-\delta}$	-10.5 K	90		144
$YBa_2(Cu_{1-x}Zn_x)_3O_{7-\delta}$		92	0.09-0.1	146
$YBa_2(Cu_{1-x}Zn_x)_3O_7$		92	$T_c(x=0.03)=55$K	147
$YBa_2(Cu_{1-x}Zn_x)_3O_{6.6}$	-22 K	90		148
$YBa_2(Cu_{1-x}Zn_x)_3O_7$		87	0.1	149
$YBa_2(Cu_{1-x}Zn_x)_3O_{6.95}$		92	$T_c(x=0.07)=20$K	150
$YBa_2(Cu_{1-x}Zn_x)_3O_{6.62}$		88.5	$T_c(x=0.02,0.06)=60,27$K	52
$YBa_2(Cu_{1-x}Ni_x)_3O_{6+y}$		94	$T_c(x=0.1)=66.3$K	141
$YBa_2(Cu_{1-x}Ni_x)_3O_{7-\delta}$		90	$T_c(x=0.05)=80$K	145
$YBa_2(Cu_{1-x}Ni_x)_3O_{6.6}$	-9.3 K	90		148
$YBa_2(Cu_{1-x}Ni_x)_3O_{7-\delta}$	-5.4 K	83		151
$La_{1.85}Sr_{0.15}(Cu_{1-x}Zn_x)O_4$		37.8	0.02-0.03	152
$La_{1.85}Sr_{0.15}(Cu_{1-x}Zn_x)O_4$		38	0.03	153
$La_{1.84}Sr_{0.16}(Cu_{1-x}Zn_x)O_4$		39	0.04	154
$La_{1.8}Sr_{0.15}(Cu_{1-x}Ni_x)O_4$		38	0.04	153
$Bi_2Sr_{0.8}La_{0.2}$ $(Cu_{1-x}Zn_x)O_y$	-4.5K	25		155
$Bi_2Sr_{0.8}La_{0.2}$ $(Cu_{1-x}Ni_x)O_y$	-2.5K	25	0.1	155

Table 4.1: The critical impurity concentration in the various experiments.

- Radthe, Levin, Schüttler and Norman[103] have taken into account the strong coupling corrections within the Eliashberg formalism. As shown in Fig. 3.2, their results are approximately reduced to prediction of the AG theory.

- Fehrenbacher[140] considered the proximity of the Fermi level to a van Hove point. Figure 4.18 shows the n_i dependence of T_c.

- Arberg and Carbotte[110] have used a more realistic band structure. They have calculated the critical temperature suppression for Born and unitary

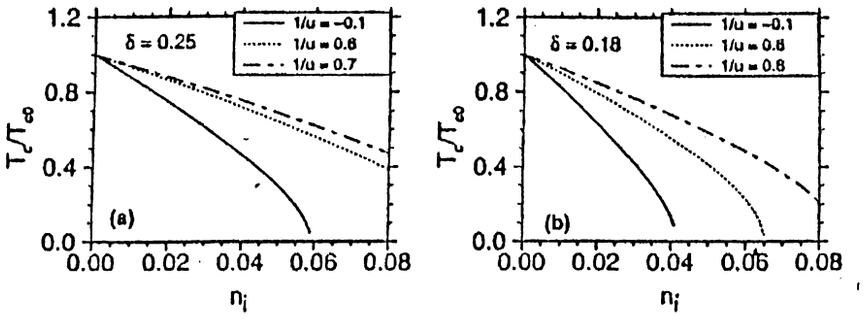

Figure 4.18: The T_c suppression for different potentials.

limits (See Fig. 4.19).

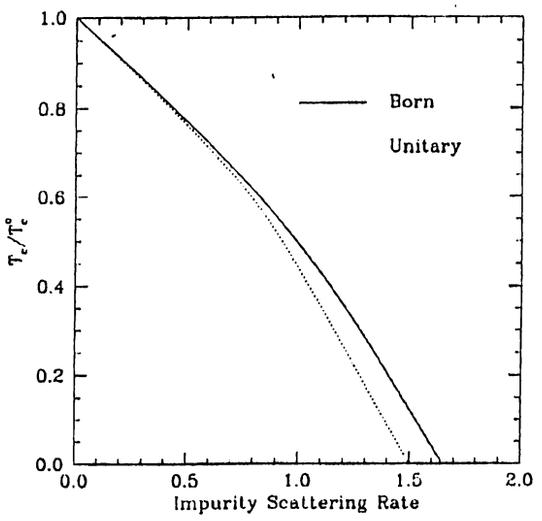

Figure 4.19: Dependence of the T_c on the impurity scattering rate for Born and unitary limits.

➤ Monthoux and Pines[106] have studied nonmagnetic impurity scattering within the spin-fluctuation model. They have calculated suppression of T_c for unitary potentials (See Fig. 4.20).

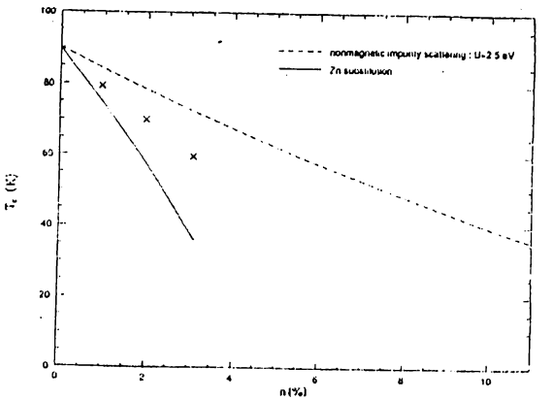

Figure 4.20: Calculated influence of Zn impurities on T_c ($\times$ indicates experimental results).

However, the discrepancy between experiment and theory remains in place. It has been suggested that[68] the traditional methods are inadequate to investigate suppression of the critical temperature T_c in the high-temperature superconductors. It may be that the main reason of breakdown of the traditional methods is due to having short coherence length ξ_0. Ref. 68 argued breakdown of standard AG type theories for short coherence lengths ($\xi_0 < 5a$).

4.7 Nonmagnetic Impurity Substitutions in the High-T_c Cuprates for Various Pairing Symmetry

In the following sections, we will present our results for isotropic s-, d- and d+s-wave superconductors.

4.7.1 Isotropic s-wave Superconductors

Isotropic s-wave solutions are obtained for the interaction terms $W_0 < 0$ and $W_1 = 0$. Figure. 4.21 shows dependence of the OP (normalized with Δ_0 which is the

OP in the absence of impurities) on the impurity concentration n_i for parameters resulting in $\xi_0 \approx 4a$ and $< n > \approx 0.8$. We can summarize the basic features of the nonmagnetic impurity effects on the isotropic s-wave superconductors as follows:

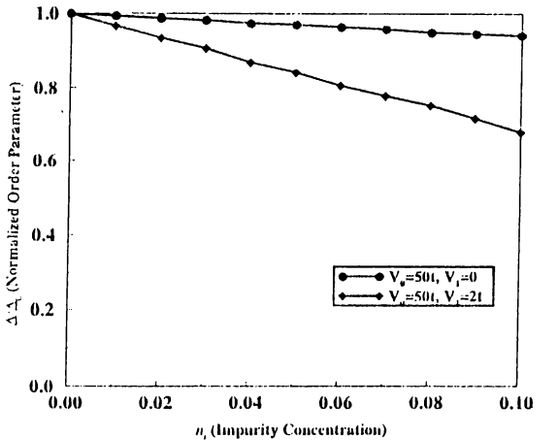

Figure 4.21: Dependence of the order parameter on the impurity concentration in the s-wave superconductors.

① The normalized OP depends on n_i linearly.

② As it has been pointed out in Chapter 3, nonmagnetic impurities have no effects on the isotropic s-wave superconductors. As shown in the Fig. 4.21 (for $V_1 = 0$) the OP is nearly constant.

③ For the finite-range potentials ($V_1 = 2t$) , the suppression is more pronounced, but it is still very small.

④ As a result, suppression of the superconductivity due to nonmagnetic impurities in the high-T_c cuprates cannot be understood in terms of the s-wave pairing symmetry.

4.7.2 d-wave Superconductors

For $W_0 > 0$ and $W_1 < 0$, d-wave symmetry is favorable. Figures. 4.22, 4.23 and 4.24 show dependence of the OP on the impurity concentration n_i.

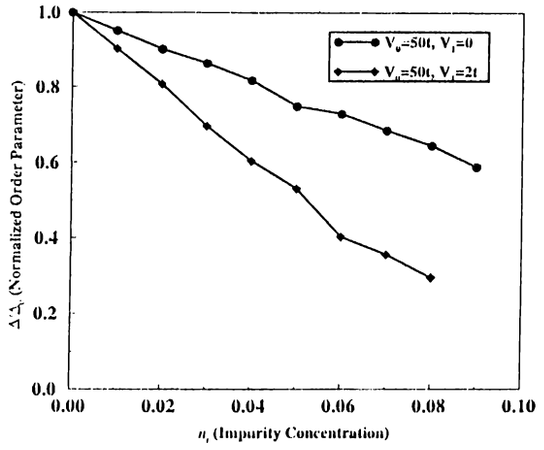

Figure 4.22: Dependence of the order parameter on the impurity concentration in the d-wave superconductors [$\xi_0 \approx 2.5a$].

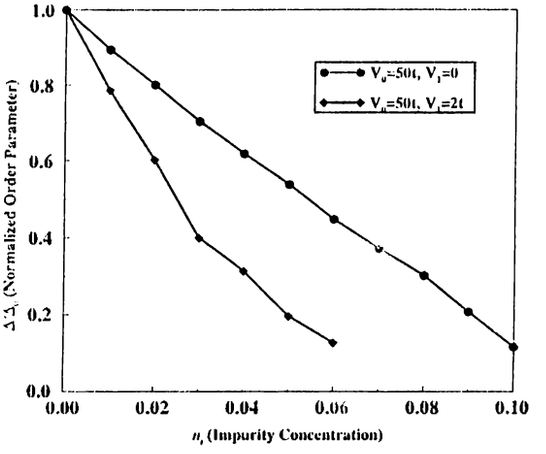

Figure 4.23: Dependence of the order parameter on the impurity concentration in the d-wave superconductors [$\xi_0 \approx 4a$].

The parameters are chosen in such a way that the coherence length becomes approximately $\xi_0 \sim 2.5a$ for Fig. 4.22, $\xi_0 \approx 4a$ for Figs. 4.23 and the electron density $< n > \approx 0.8$ (We use $W_0 = -W_1 = -1.08t$, $\mu = -0.5t$ and $k_B T = 0.005t$). We can summarize the basic features of the nonmagnetic impurity effects on the

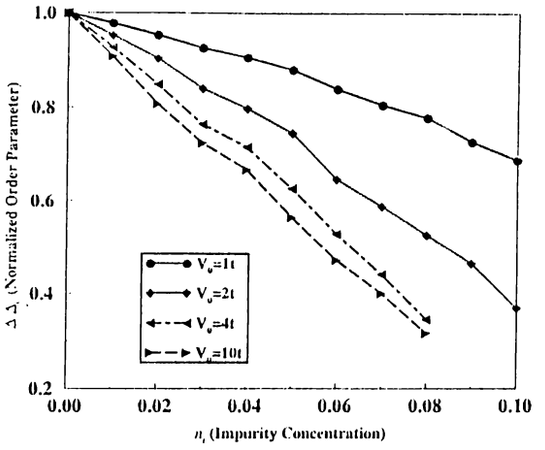

Figure 4.24: Dependence of the order parameter on the impurity concentration for different values of impurity potentials in the d-wave superconductors [$\xi_0 \approx 4.5a$].

d-wave superconductors as follows:

① The normalized OP depends on linearly n_i as in the experiments.

② Superconductivity is suppressed very rapidly and it vanishes at a critical value of the impurity concentration $n_c \approx 0.1$ for $\xi_0 \approx 4a$ (See Fig. 4.23). This is in quite good agreement with experimental data $n_c \approx [0.8 - 0.12]$ for YBCO compounds.

③ The finite-ranged potential can be proposed to explain the differences between the Zn and Ni impurities (See Fig. 4.23).

④ The differences between Zn and Ni can also be understood by taking different potentials strength for these ions (See Fig. 4.24).

4.7.3 s+d-wave Superconductors

As has been discussed in Chapter 3, due to orthorhombicity of the YBCO compound, admixture of s and d-waves is always possible. Figure 4.25 shows dependence of the OP on the impurity concentration n_i for s+d-wave superconductors. The parameters are chosen to result in $\xi_0 \approx 4a$ and $< n > \approx 0.8$.

It should be noted that due to a-b plane anisotropy, we take $t_x = 1t$ and $t_y = 1.55t$.

We can summarize the basic features of the nonmagnetic impurity effects on the s+d-wave superconductors as follows:

① The normalized OP depend on n_i linearly for small values of the impurity concentration. However, at large values of n_i the OP has a tail. This can be understood by considering s-wave component of the OP is suppressed slowly compared to d-wave component.

② In this pairing symmetry, the critical impurity concentration is about 0.1 in agreement with experiments.

③ The differences between Zn and Ni can be understood by noticing that Ni substitution leads to a orthorhombic-tetragonal transition. Therefore, we can assume that Ni has d-wave symmetry while Zn has s+d-wave symmetry. Since s+d-wave is more sensitive to the impurities than d-wave, Zn suppresses the superconductivity more rapidly than Ni.

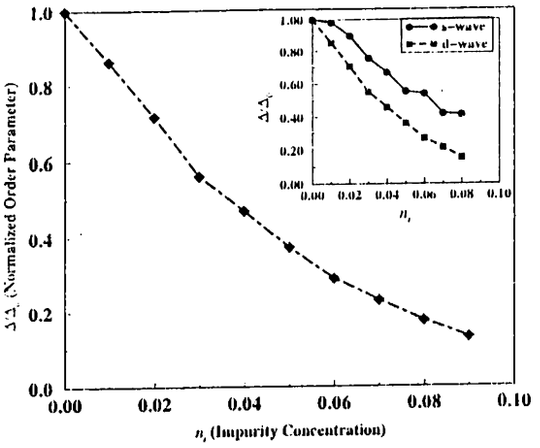

Figure 4.25: Dependence of the order parameter on the impurity concentration in the s+d-wave superconductors.

Chapter 5

RESULTS AND CONCLUSIONS

We have reviewed the properties of the high-T_c cuprates, the Bogoliubov-de Gennes equations (BdG) and the impurity effects on isotropic and anisotropic superconductors. Nonmagnetic impurity substitutions in high-T_c oxide superconductors have been investigated by solving BdG equations on two-dimensional a square lattice. We can summarize our results as follows:

❑ The critical concentration is YBCO is found to be around $n_c \sim 0.1$. This is in agreement with experimental results where $n_c \sim [0.08 - 0.1]$.

❑ Differences between Zn and Ni substitutions can be understood

❶ by taking finite-ranged impurity potentials,

❷ by taking different potential strengths for Zn and Ni,

❸ by considering that impurity substitution leads to a phase transition for Ni from orthorhombic to tetragonal phase.

❑ Our results support the d-wave order parameter symmetry, and strongly reject s-wave. We can not say anything about the other pairing symmetries such as extended s, p, s+id.

❑ Considering the orthorhombicity of the YBCO materials, we have found that admixture of s and d waves is possible. This type of symmetry is recently proposed for YBCO materials in Ref. 135.

Bibliography

[1] E. Waxwell, Isotope Effect in the Superconductivity of Mercury, Phys. Rev. **78**, 477 (1950).

[2] Reynolds *et. al.*, Superconductivity of Isotopes of Mercury, Phys. Rev. **78**, 487 (1950).

[3] J. Barden, L. N. Cooper, and J. R. Schrieffer, Theory of Superconductivity, Phys. Rev. **108**, 1175 (1957).

[4] Leon N. Cooper, Bound Electron Pairs in a Degenerate Fermi Gas, Phys. Rev. **104**, 1189 (1956).

[5] B. S. Deaver *et. al.*, Experimental Evidence for Quantized Flux in Superconducting Cylinders, Phys. Rev. Lett. **7**, 43 (1961).

[6] R. Doll and M. Nöbauer, Experimental Proof of Magnetic Flux Quantization in a Superconducting Ring, Phys. Rev. Lett. **7**, 51 (1961).

[7] Superconductivity, edited by R. D. Parks, (M. Dekker, New York, 1969).

[8] P. G. de Gennes, Superconductivity of Metals and Alloys (Addison-Wesley, Readings, MA, 1989).

[9] M. Tinkham, Introduction to Superconductivity, (McGraw-Hill, New York, 1996).

[10] C. P. Poole, Jr., *et. al.*, Superconductivity, (Academic Press, 1995).

[11] Z. Gedik, High-T_c Superconductivity, (M. S. Thesis, Bilkent University, Ankara, 1989).

[12] G. Vidali, Superconductivity (The Next Revolution), (Cambrigde, 1993).

[13] V.L. Ginzburg, E.A. Andryushin, Superconductivity, (World Scientific, 1994).

[14] M. Cyrot, D. Pavuna, Introduction to Superconductivity and High-T_c Materials, (World Scientific, 1992).

[15] J. G. Bednorz and K. A. Müller, Z. Phys. B **64**, 189 (1986).

[16] J. G. Bednorz and K. A. Müller, The Discovery of a Class of High-Temperature Superconductors, Science **237**, 1133 (1987).

[17] N. M. Plakida, High-Temperature Superconductivity (Experiment and Theory), (Springer, Berlin, 1995).

[18] J. Gonzalez *et. al.*, Quantum Electron Liquids and High-T_c Superconductivity (Experiment and Theory), (Springer, Berlin, 1995).

[19] D. M. Ginsberg, Introduction, History, and Overview of High Temperature Superconductivity, in Physical Properties of High Temperature Superconductors I, edited by D. M. Ginsberg, (World Scientific, 1989).

[20] B. L. Chamberland, Historical Introduction and Crystal Chemistry of Oxide Superconductors, in Chemistry of Superconductor Materials, edited by T. A. Vanderah, (Noyes, 1992).

[21] V. Z. Kresin *et. al.*, Mechanism of Conventional and High-T_c Superconductivity, (Oxford, 1993).

[22] P. W. Anderson, Theory of Dirty Superconductors, J. Phys. Chem. Solids **11**, 26 (1959).

[23] M. K. Wu *et. al.*, Superconductivity at 93 K in a New Mixed-Phase Y-Ba-Cu-O Compound System at Ambient Pressure, Phys. Rev. Lett. **58**, 908 (1987).

[24] V. Kresin and S. Wolf, Solid State Commun. **63**, 1141 (1987).

[25] V. Kresin *et. al.*, J. Supercond. **1**, 327 (1988).

[26] D. Pines, Lecture Notes of Summer School on Condensed Matter Physics, held on 17-22 June 1996, Bilkent University, Ankara, Turkey.

[27] A. J. Leggett, Lecture Notes of Summer School on Condensed Matter Physics, held on 17-22 June 1996, Bilkent University, Ankara, Turkey.

[28] A. Santoro, in High Temperature Superconductivity, edited by J. W. Lynn, (Springer, New York, 1990).

[29] P. B. Littlewood, Phenomenology of High-Temperature Superconductors, in Strongly Interacting Fermions and High-T_c Superconductivity, edited by B. Doucot and J. Z. Justin, (Elsevier, 1995).

[30] B. Batlogg, Selected Experiments on High-T_c Cuprates, in High-Temperature Superconductivity Proceedings, edited by K. K. Bedell *et. al.*, (Addison-Wesley, 1990).

[31] H. R. Ott, Unusual (Anomalous) Properties of the Normal and Superconducting State of Cu-Oxides, in Physics of High-Temperature Superconductors, edited by S. Mackawa and M. Sato, (Springer, Berlin, 1992).

[32] M. Takigawa *et. al.*, Spin Susceptibility in Superconducting $YBa_2Cu_3O_7$ from ^{63}Cu Knight Shift, Phys. Rev. B **39**, 7371 (1989).

[33] S. E. Barrett *et. al.*, Anomalous Behavior of Nuclear Spin-Lattice Relaxation Rates in $YBa_2Cu_3O_7$ Below T_c, Phys. Rev. Lett. **66**, 108 (1991).

[34] A. A. Abrikosov *et. al.*, Methods of Quantum Field Theory in Statistical Physics, (Dover, New York, 19963), chapter 7.

[35] A. A. Abrikosov, Fundamentals of the Theory of Metals, (North-Holland, Amsterdam, 1988), Chapter 21.

[36] M. Acquarone, Effects of Substitutions in the CuO Plane of High-T_c Superconductors: The Theoretical Aspects, in High-Temperature Superconductivity models and Measurements, edited by M. Acquarone, (World Scientific, 1996).

[37] M. Acquarone, Diamagnetic Substitution Effects in Copper Perovskites: The Italian Contribution, in High-Temperature Superconductivity models and Measurements, edited by M. Acquarone, (World Scientific, 1996).

[38] M. D'astuto and M. Acquarone, Effects Substitutions on the Copper Site in $Nd_{2-y}Ce_yCuO_4$ in Copper Perovskites, in High-Temperature Superconductivity models and Measurements, edited by M. Acquarone, (World Scientific, 1996).

[39] J. T. Markert *et. al.*, Rare Earth and Other Substitutions in High Temperature Oxide Superconductors, in Physical Properties of High Temperature Superconductors I, edited by D. M. Ginsberg, (World Scientific, 1989).

[40] L. H. Greene and B. G. Bagley, Oxygen Stoichiometric Effects and Related Atomic Substitutions in the High-T_c Cuprates, in Physical Properties of High Temperature Superconductors II, edited by D. M. Ginsberg, (World Scientific, 1990).

[41] J. M. Tarascon and B. G. Bagley, Cationic Substitutions in the High-T_c Superconductors, in Chemistry of Superconductor Materials, edited by T. A. Vanderah, (Noyes, 1992).

[42] D. R. Harshman and A. P. Mills, Concerning the Nature of High-T_c Superconductivity: Survey of Experimental Properties and Implications for Interlayer Coupling, Phys. Rev. B **45**, 10684 (1992).

[43] G. Xiao *et. al.*, High-Temperature Superconductivity in Tetragonal Perovskite Structure: Is Oxygen-Vacancy Order Important, Phys. Rev. Lett. **60**, 1446 (1988).

[44] D. Esteve *et. al.*, Europhys. Lett. **3**, 1237 (1987).

[45] C. E. Gough *et. al.*, Nature **326**, 855 (1987).

[46] J. R. Kirtley, Int. J. Mod. Phys. B **4** , 201 (1990).

[47] M. Gurvitch *et. al.*, Reproducible Tunneling Data or Chemically Etched Single Crystals of $YBa_2Cu_3O_7$, Phys. Rev. Lett. **63**, 1008 (1989).

[48] H. F. C. Hoevers *et. al.*, Physica C **152**, 105 (1988).

[49] H. Keller, Muon Spin Rotation Experiments High-T_c Superconductors, in in Earlier and Recent Aspects of Superconductivity, edited by J. G. Bednorz and K. A. Müller, (Springer, Berlin, 1990).

[50] Z. P. Han *et. al.*, Comparative μSR and NMR Studies of the Doping Effects in $Y(Ba_{1-x}La_x)_2Cu_3O_7$, Physica C **235-240**, 1723 (1994).

[51] C. Bucci, Investigation of Magnetic properties in High-T_c oxides by Muon Spin Rotation, in Superconductivity (From Basic Physics to the latest developments), edited by P. N. Butcher and Y. Lu, (World Scientific, 1995).

[52] C. Bernhard *et. al.*, Suppression of the Superconducting Condensate in the High-T_c Cuprates by Zn Substitution and Overdoping: Evidence for an Unconventional Pairing State, Phys. Rev. Lett. **77**, 2304 (1996).

[53] I. O. Kulik, Contraction of Atomic Orbitals in the Oxygen Anion Network and Superconductivity in Metal Oxide Compounds, Tr. J. of Physics **20**, 627 (1996).

[54] This volume is devoted to discussion of symmetry of order parameter in high-temperature superconductors, Tr. J. of Physics **20**, (1996).

[55] D. Scalapino, Phys. Rep. **250**, 392 (1995).

[56] P. Monthoux, A. Balatsky and D. Pines, Weak-Coupling Theory of High-Temperature Superconductivity in the Antiferromagnetically Correlated Copper Oxides, Phys. Rev. B **46**, 14803 (1992).

[57] J. Van Harlingen, Phase-Sensitive Tests of the Pairing State in the High-Temperature Superconductors-Evidence for $d_{x^2-y^2}$ Symmetry, Rev. Mod. Phys. **67**, 515 (1995).

[58] B. G. Levi, In High-T_c Superconductors, Is d-Wave the New State?, Physics Today **46**(5), 17 (1993).

[59] J. F. Annett *et. al.*, The Pairing State of $YBa_2Cu_3O_{7-\delta}$, in Physical Properties of High Temperature Superconductors II, edited by D. M. Ginsberg, (World Scientific, 1990).

[60] S. E. Barrett *et. al.*, ^{63}Cu Knight Shifts in the Superconducting State of $YBa_2Cu_3O_{7-\delta}$ ($T_c = 90K$), Phys. Rev. B **42**, 6283 (1990).

[61] T. R. Chien *et. al.*, Effect of Zn Impurities on the Normal-State Hall Angle in Single-Crystal $YBa_2Cu_{3-x}Zn_xO_{7-\delta}$, Phys. Rev. Lett. **67**, 2088 (1991).

[62] G. Reiter *et. al.* (editors), Dynamics of Magnetic Fluctuation in High-Temperature Superconductors, (Plenum, New York, 1991).

[63] N. N. Bogoliubov, Sov. Phys. JETP **7**, 41 (1958).

[64] N. N. Bogoliubov, On a New Method in the Theory of Superconductivity , in Selected Works Of N. N. Bogoliubov, edited by N.N. Bogoliubov and A. M. Gurbetov, (Gordon and Breach Science PubNew York ,1991).

[65] T. Xiang and J. M. Wheatley, Disorder Effect in Low Dimensional Superconductors, Physica C **235**, 2409 (1994).

[66] T. Xiang and J. M. Wheatley, Nonmagnetic Impurities in Two-dimensional Superconductors, Phys. Rev. B **51**, 11721 (1995).

[67] M. Franz, C. Kallin, and A. J. Berlinsky, Impurity Scattering and Localization in d-wave Superconductors, Phys. Rev. B **54**, R6897, (1996).

[68] M. Franz *et. al.*, Critical Temperature and Superfluid Density Suppression in Disordered High-T_c Cuprate Superconductors, preprint cond-mat/9610167.

[69] P. H. C. Magnee *et. al.*, Experimental Determination of the Quasi-particle Decay Length ξ_{Sm} in a Superconducting Quantum Wells, preprint cond-mat/9502038.

[70] A. Martin and C. J. Lambert, Self-consistent Current-voltage Characteristics of Superconducting Nano-structures, preprint cond-mat/9504105.

[71] R. J. Troy and Alan T. Dorsey, Self-consistent Microscopic Theory of Surface Superconductivity, Phys. Rev. B **51**, 11728 (1995).

[72] Yong Wang and A. H. MacDonald, Mixed-state Quasiparticle Spectrum for d-wave Superconductors, Phys. Rev. B **52**, R3876 (1995).

[73] J. D. Shore *et. al.*, Density of States in a Vortex Core and the Zero-Bias Tunneling Peak, Phys. Rev. Lett. **62**, 3089 (1989).

[74] Francois Gygi and Michael Schluter, Electronic Tunneling into a Isolated Vortex in a Clean Type-II Superconductor, Phys. Rev. B **41**, 822 (1990).

[75] Francois Gygi and Michael Schluter, Angular Band Structure of a Vortex Line in a Type-II Superconductor, Phys. Rev. Lett. **63**, 1820 (1990).

[76] Francois Gygi and Michael Schluter, Self-consistent Electronic Structure of a Vortex Line in a Type-II Superconductor, Phys. Rev. B **43**, 7609 (1991).

[77] Yu-Dong Zhu *et. al.*, Electronic Structure of a Vortex Line in a Type-II Superconductors: Effect of Atomic Crystal Fields, Phys. Rev. B **51**, 1105 (1995).

[78] P. I. Soininen *et. al.*, Structure of a Vortex Line in a d-x^2-y^2 Superconductors, Phys. Rev. B **50**, 13883 (1994).

[79] C. Kallin *et. al.*, Vortices in d-wave Superconductors, J. Phys. Chem. Solid **56**, 1619 (1995).

[80] M. E. Zhitomirsky and M. B. Walker, Electronic States on a Twin Boundary of a d-wave Superconductors, preprint cond-mat/9705202.

[81] D. L. Feder *et. al.*, Twin Boundaries in d-wave Superconductors, preprint cond-mat/9705139.

[82] L. D. Landau and E. M. Lifshitz, Quantum Mechanics (Non-relativistic Theory), section 64, (Pergaman, 1987).

[83] G. C. Wick, The Evaluation of the Collision Matrix, Phys. Rev. **80**, 268 (1950).

[84] A. A. Abrikosov and L. P. Gor'kov, On the Theory of Superconducting Alloys: The Electrodynamics of Alloys at Absolute Zero, Sov. Phys. JETP 8, 1090 (1959).

[85] E. A. Lynton *et. al.*, J. Phys. Chem. Solids **3**, 165 (1957).

[86] G. Chanin *et. al.*, Impurity Effects on the Superconducting Critical Temperature of Indium and Aluminum, Phys. Rev. **114**, 719(1959).

[87] K. Maki, Gapless Superconductivity, in Superconductivity, edited by R. D. Parks, (M. Dekker, New York, 1969).

[88] P. G. de Gennes, Boundary Effects in Superconductors, Rev. Mod. Phys. **36**, 225 (1964).

[89] A. A. Abrikosov and L. P. Gor'kov,Contribution to the Theory of Superconducting Alloys with Paramagnetic Impurities, Sov. Phys. JETP **12**, 1243 (1961).

[90] S. Skalski *et. al.*, Properties of Superconducting Alloys Containing Paramagnetic Impurities, Phys. Rev. **136**, A1500 (1964).

[91] V. L. Pokrovskii, Sov. Phys. JETP **13**, 100,447,628 (1961).

[92] D. Markowitz and L. P. Kadanoff, Effects of Impurities upon Critical Temperature of Anisotropic of the Superconductors, Phys. Rev. **131**, 563 (1963).

[93] P. Hohenberg, Anisotropic Superconductors with Nonmagnetic Impurities, Sov. Phys. JETP **18**, 834 (1964).

[94] J. R. Clem, Effects of Nonmagnetic Impurities upon Anisotropic of the Superconducting Energy Gap, Phys. Rev. **148**, 392 (1966).

[95] A. A. Abrikosov, Influence of the gap Anisotropy on Superconducting Properties, Physica C **214**, 107 (1993).

[96] A. A. Abrikosov, On the Nature of the Order Parameter in HTSC and Influence of Impurities, Physica C **244**, 243(1995).

[97] G. D. Mahan, Many-Particle Physics, (Plenum Press, New York, 1990).

[98] O. T. Valls and M. T. Beal-Monod, Effect of Interaction Anisotropy on the Superconducting Transition Temperature, Phys. Rev. B **51**, 8438 (1995).

[99] M. T. Beal-Monod and O. T. Valls, T_c Enhancement Due to Anisotropy in the Pairing Interaction, Europhys. Lett. **30**, 415 (1995).

[100] V. F. Elesin *et. al.*, Analysis of Experiments on the Ion Irradiation of $YBa_2Cu_3O_{7-x}$ Films: d pairing or anisotropic s pairing?, Sov. Phys. JETP **83**, 395 (1996).

[101] E. M. Jackson *et. al.*, Radiation-Induced T_c Reduction and Pair Breaking in High-T_c Superconductors, Phys. Rev. Lett. **74**, 3033 (1996).

[102] L. S. Borkowski and P. J. Hirschfeld, Distinguishing d-wave Superconductors from Highly Anisotropic s-wave Superconductors, Phys. Rev. B **49**, 15404 (1994).

[103] R. J. Radtke *et. al.*, Predictions for Impurity-Induced T_c Suppression in the High-Temperature Superconductors, Phys. Rev. B **48**, 653 (1993).

[104] R. Fehrenbacher and M. R. Norman, Gap Renormalization in Dirty Anisotropic Superconductors: Implications for the Order Parameter of the Cuprates, Phys. Rev. B **50**, 3495 (194).

[105] P. J. Hirschfeld and N. Goldenfeld, Effect of Strong Scattering on the Low-Temperature Penetration Depth of a d-wave Superconductor, Phys. Rev. B **48**, 4219 (1993).

[106] P. Mouthoux and D. Pines, Spin-Fluctuation-Induced Superconductivity and Normal-State Properties of $YBa_2Cu_3O_7$, Phys. Rev. B **49**, 4261 (1994).

[107] S. V. Pokrovsky and V. L. Pokrovsky, Energy Gap Induced by Impurity Scattering: New Phase in Anisotropic Superconductors, Phys. Rev. Lett. **75**, 1150 (1995).

[108] S. V. Pokrovsky and V. L. Pokrovsky, Density of States and Order Parameter in Dirty Anisotropic Superconductors, Phys. Rev. B **54**, 13275 (1996).

[109] G. Preosti and P. Muzikar, Superconducting Order Parameters with Sign Changes: The Density of States and Impurity Scattering, Phys. Rev. B **54**, 3489 (1996).

[110] P. Arberg and J. P. Carbotte, Effect of the Impurity Scattering on the Zero-Temperature Penetration Depth in d-$x^2 - y^2$ symmetry.,

[111] A. A. Golubov and I. I. Mazin, Effect of Magnetic and Nonmagnetic Impurities on Highly Anisotropic Superconductivity , Phys. Rev. B **55**, 15146 (1997).

[112] M. T. Beal-Monod and K. Maki, Impurity Scattering in d+s Wave Superconductivity, Europhys. Lett. **33**, 309 (1996).

[113] H. Kim and E. J. Nicol, Effect of Impurity Scattering on a (d+s)-wave Superconductor , Phys. Rev. B **52**, 13576 (1995).

[114] J. E. Hirsch *et. al.*, Pairing Interaction in Two-Dimensional CuO_2, Phys. Rev. Lett. **60**, 1668 (1988).

[115] N. E. Bickers, D. J. Scalapino and T. Scallettar, Int. J. Mod. Phys. B **1**, 687 (1987).

[116] P. Mouthoux, A. V. Balatsky and D. Pines, Phys. Rev. B **46**, 961 (1992).

[117] Y. J. Kim, Pairing in the Bogoliubov-de Gennes Equations, preprint cond-mat/9701102.

[118] A. Buzdin and A. Varlamov, Meeting No Resistance, Quantum September/October, 6 (1991).

[119] Y. J. Kim and A. W. Overhauser, Magnetic Impurities in Superconductors: A Theory with Different Predictions, Phys. Rev. B **49**, 15799 (1994).

[120] J. R. Schrieffer, The Pairing Theory-Its Physical Basis and Its Consequences, in Physics of High-Temperature Superconductors, edited by S. Maekawa and M. Sato, (Springer, Berlin, 1992).

[121] J. M. Byers, M. E. Flatte and D. J. Scalapino, Influence of Gap Extrema on the Tunneling Conductance Near an Impurity in an Anisotropic Superconductor , preprint cond-mat/9306048.

[122] A. J. Millis, S. Sachdev and C. M. Varma, Inelastic Scattering and Pair Breaking in Anisotropic and Isotropic Superconductors, Phys. Rev. B **37**, 4975 (1988).

[123] P. Fulde and G. Zwicknagl, Pair Breaking in Superconductors, in in Earlier and Recent Aspects of Superconductivity, edited by J. G. Bednorz and K. A. Müller, (Springer, Berlin, 1990).

[124] Yong Wang and A. H. MacDonald, Mixed-state penetration depths in s-wave and d-wave superconductors, preprint cond-mat/9607094.

[125] A. V. Balatsky, A. Rosengren and B. L. Altshuler, Impurities and Quasi-One Dimensional Transport in a d-wave Superconductors, preprint cond-mat/9311004.

[126] R. Micnas, J. Ranninger and S. Robaszkiewicz, Superconductivity in Narrow-band with Local Nonretarded Attractive interactions, Rev. Mod. Phys. **62**, 113 (1990).

[127] M. T. Beal-Monod and K. Maki, Low Temperature Thermal Conductivity in d+s Wave Superconductivity, Physica C **265**, 309 (1996).

[128] K. Maki and M. T. Beal-Monod, Anisotropic d+s Wave Superconductivity, Physics Letters A **208**, 365 (1995).

[129] Ye Sun and K. Maki, Impurity Effects in d+s Wave Superconductivity, Physica C **265**, 309 (1996).

[130] R. Fehrenbacher and M. R. Norman, Can Impurity Effects Help to Identify the Symmetry of the Order Parameter of the Cuprates?, preprint cond-mat/9405030.

[131] Mi-Ae Park, M. H. Lee and Yong-Jihn Kim, Impurity Scattering in a d-wave Superconductor, preprint cond-mat/9707235.

[132] M. V. Sadovskii, A. I. Posazhennikova, Disorder Effects in Superconductors with Anisotropic Pairing: From Cooper Pairs to Compact Bosons , preprint cond-mat/9612188.

[133] B. C. den Hertog and M. P. Das, Local Moment Formation in Zinc Doped Cuprates, preprint cond-mat/9702190.

[134] P. K. Mohanty and A. Taraphder, Order Parameter Symmetry in Doped YBCO Systems, preprint cond-mat/9703180.

[135] K. A. Kouznetsov *et. al.*, C-axis Josephson Tunneling Between $YBa_2Cu_3O_{7-\delta}$ and Pb: Direct Evidence for Mixed Order Parameter Symmetry in the High-T_c Superconductors, preprint cond-mat/9705283.

[136] D. N. Basov *et. al.*, In-Plane Anisotropy of the Penetration Depth in $YBa_2Cu_3O_{7-x}$ and $YBa_2Cu_3O_8$ Superconductors , Phys. Rev. Lett. **74**, 598 (1995).

[137] S. B. Nam, Pairing Theory of High and Low Temperature Superconductors, preprint cond-mat/9707017.

[138] P. Chaundhari, Some Implications of a Short Coherence Length in High-Temperature Superconductors, in Physics of High-Temperature Superconductors, edited by S. Mackawa and M. Sato, (Springer, Berlin, 1992).

[139] E. R. Ulm *et. al.*, Magnetic Penetration Depth in Ni- and Zn-Doped $YBa_2(Cu_{1-x}\mathcal{M}_x)_3O_7$, Phys. Rev. B **51**, 9193 (1995).

[140] R. Fehrenbacher, Nonmagnetic Impurity Scattering in a d-x^2-y^2 Superconductors near a Van Hove Point: Zn versus Ni in the Cuprates, Phys. Rev. Lett. **77**, 1849 (1996).

[141] G. Xiao *et. al.*, Effects of Transition-Metal Elements on the Superconductivity of Y-Ba-Cu-O, Phys. Rev. B **35**, 8782 (1987).

[142] B. Jayaram *et. al.*, anomalously Large T_c Depression by Zn Substitution in Y-Ba-Cu-O, Phys. Rev. B **38**, 2903 (1988).

[143] M. Mehbod *et. al.*, Influence of Zn Impurities on the Superconducting Y-Ba-Cu-O Compound, Phys. Rev. B **38**, 11813 (1988).

[144] C. T. Rose *et. al.*, Normal and Superconductive Properties of Zinc-Doped $YBa_2Cu_3O_7$ Thin Films, in Physics and Materials Science of High Temperature Superconductors, edited by R. Kossowky, (Kluwer, 1992).

[145] A. M. Balagurov and J. Piechota, Neutron Powder Diffraction Studies of $YBa_2(Cu_{1-x}\mathcal{M}_x)_3O_{7-\delta}$ with $\mathcal{M}$ =^{57}Fe,^{58}Ni , in Physics and Materials Science of High Temperature Superconductors, edited by R. Kossowky, (Kluwer, 1992).

[146] F. Bridges *et. al.*, Distorted Local Environment Around Zn on $Cu(2)$ Sites in $YBa_2Cu_3O_7$: An x-ray-absorption Study, Phys. Rev. B **48**, 1267 (1993).

[147] A. Janossy *et. al.*, Suppression of the Superconducting Gap and the Spin-fluctuation Gap of $YBa_2Cu_3O_y$ ($y = 7.0$ and 6.76), Phys. Rev. B **50**, 3442 (1994).

[148] P. Mendels *et. al.*, Macroscopic Magnetic Properties Of Ni and Zn Substituted $YBa_2Cu_3O_x$, Physica C **235-240** 1595 (1995).

[149] S. Zagoulaev *et. al.*, Magnetic and Transport Properties Of Zinc-Doped $YBa_2Cu_3O_7$ in Normal State, Phys. Rev. B **52**, 10474 (1995).

[150] D. J. C. Walker *et. al.*, Transport Properties Of Zinc-Doped $YBa_2(Cu_3O_{7-\delta}$ Thin Films, Phys. Rev. B **51**, 15653 (1995).

[151] A. Odagawa and Y. Enomoto, Normal Resistivity and Superconducting Properties on $YBa_2(Cu_{1-x}Ni_x)_3O_{7-\delta}$ Films, Physica C **248** 162 (1995).

[152] G. Xiao *et. al.*, Correlation Between Superconductivity and Normal-State Properties in the $La_{1.8}Sr_{0.15}(Cu_{1-x}Zn_x)O_4$ System, Phys. Rev. B **39**, 315 (1989).

[153] G. Xiao *et. al.*, Magnetic Pair-Breaking Effects: Moment Formation and Critical Doping Level in Superconducting $La_{1.8}Sr_{0.15}(Cu_{1-x}A_x)O_4$ Systems (A=Fe,Co,Ni,Zn,Ga,Al), Phys. Rev. B **39**, 315 (1989).

[154] N. Momono *et. al.*, Low-Temperature Electronic Specific Heat of $La_{2-x}Sr_xO_4$ and $La_{2-x}Sr_x(Cu_{1-y}Zn_y)O_4$. Evidence for a d wave Superconductor , Physica C **233** 395 (1994).

[155] Z. Mao, *et. al.*, Effect of Ni and Zn Substitutions for Cu in the 25K Phase of Bi-Sr-La-Cu-O Superconductors, Jpn. J. Appl. Phys. Part I **35**, 3383 (1996).